Khulan Bayarsaikhan, BSc

Vibration damping of a height adjustable desk by active noise control

Master's Thesis

to achieve the university degree of

Diplom-Ingenieur

Master's degree programme: Electrical Engineering

submitted to

Graz University of Technology

Supervisor

Ass-Prof. Dipl.-Ing. Dr. Martin Steinberger

Institute of Automation and Control

Head: Univ.-Prof. Dipl.-Ing. Dr.techn. Martin Horn

Graz, May 2018

Statutory Declaration

I declare that I have authored this thesis independently, that I have not used other than the declared sources/resources, and that I have explicitly indicated all material which has been quoted either literally or by content from the sources used. The text document uploaded to TUGRAZ online is identical to the present master‘s thesis.

Eidesstattliche Erklärung

Ich erkläre an Eides statt, dass ich die vorliegende Arbeit selbstständig verfasst, andere als die angegebenen Quellen/Hilfsmittel nicht benutzt, und die den benutzten Quellen wörtlich und inhaltlich entnommenen Stellen als solche kenntlich gemacht habe. Das in TUGRAZ online hochgeladene Textdokument ist mit der vorliegenden Dissertation identisch.

Graz, am	(Unterschrift)

Abstract

The performance of digital signal processors (DSP)s or field programmable gate arrays (FPGA)s improved over the last decades, which allows to use algorithms with high computational complexity. One example of usage is an algorithm of active noise control, which in general requires high computation in a real time system. The active noise control is used in many applications such as in manufacturing, industrial operations and consumer products, e.g. headphones.

In this thesis, the vibration of a height adjustable desk is damped using an active noise control (ANC). Since the vibration of the desk is a broadband signal, a single-channel Filtered-x LMS algorithm is applied as ANC. The single-channel filtered-x least mean square (FxLMS) algorithm consists two inputs and one output. The FxLMS algorithm cancels a primary source vibration by producing a secondary signal. This secondary signal is the output of the algorithm and it is calculated based on the values of the inputs.

In the experiment, two 360° vibro-speakers are used as a primary and secondary source shaker. A first acceleration sensor measures the vibration of the primary source shaker. A second acceleration sensor measures the error residue of the ANC. Both measurements are used as inputs for the FxLMS.

The ANC is applied to a narrowband and a broadband signal. For the narrowband signal, the FxLMS algorithm was able to damp the plate vibration at the error sensor position and the noise in the air is decreased by up to $20dB$. For the broadband signal, the FxLMS algorithm was able to damp the plate vibration by up to $20dB$ at the error sensor position and the noise in the air is decreased by $2dB$.

Kurzfassung

Die Rechenleistung von DSPs oder FPGAs wurde in den letzten Jahrzehnten kontinuierlich verbessert, was den Einsatz von Algorithmen mit hoher Rechenkomplexität ermöglichte. Die aktive Lärmkontrolle in einem Echtzeitsystem ist ein Beispiel für solch einen rechenintensiven Algorithmus. Der aktive Schallschutz kommt in vielen Anwendungen zum Einsatz, z.B. in der Fertigung, in Industriebetrieben und bei Konsumgütern wie etwa Kopfhörern.
In dieser Arbeit wird die Schwingung eines höhenverstellbaren Tisches mit ANC gedämpft. Da die Schwingung eines höhenverstellbaren Tisches ein breitbandiges Signal ist, wird als ANC ein einkanaliger Filtered-x-LMS-Algorithmus verwendet. Das verwendete System hat dabei zwei Eingänge und einen Ausgang. Der FxLMS-Algorithmus hebt die Primärschwingung auf, indem er ein Sekundärsignal erzeugt. Dieses Sekundärsignal ist der Ausgang des Algorithmus und wird aus den Werten der Eingänge berechnet.
Im Experiment werden zwei 360° Vibrations-Lautsprecher als primäre und sekundäre Vibrationsquelle verwendet. Der erste Beschleunigungssensor misst die Schwingung der primären Vibrationsquelle, der zweite Beschleunigungssensor misst den verbleibenden Fehler des ANC. Beide Messungen werden als Eingänge für das FxLMS verwendet.
Der Algorithmus wird auf ein schmalbandiges und breitbandiges Signal angewendet. Für das schmalbandige Signal konnte der FxLMS-Algorithmus die Plattenschwingung an der Fehlersensorposition dabei dämpfen und der Lärm in der Luft wird um bis zu $20dB$ reduziert. Für das Breitbandsignal konnte der FxLMS-Algorithmus die Plattenschwingung an der Fehlersensorposition um bis zu $20dB$ dämpfen und der Lärm in der Luft wird um $2dB$ gedämpft.

Acknowledgement

I would like to thank to my thesis supervisor Professor Martin Steinberger for his good advice and guidance in writing this master thesis. I also thank the colleagues from LOGICDATA, Mathias Maier, Clemens Treichler, and Christoph Baumgartner, who all advised me during my thesis. Special thanks to my team leader Aljaz Bernhard for supported me during my study.
It was a big journey to do my master degree in Austria and during this journey many people helped and supported me. Therefore , I would like to thank to my parents, my friend Andreas Zehetner and his family.

Graz, May 2018 Khulan Bayarsaikhan

Contents

List of Abbreviations

ADC	Analog to Digital Converter
ANC	Active Noise Control
DAC	Digital to Analog Converter
dB	Decibel
DSP	Digital Signal Processor
FFT	Fast Fourier Transform
FIR	Finite Impulse Response
FxLMS	Filtered Least Mean Square
IIR	Infinite Impulse Response
LMS	Least Mean Square
MSE	Mean Square Error
RLS	Recursive Least mean Square
RMS	Root Mean Square
SNR	Signal Noise Ratio
SP	Secondary Path
SPL	Sound Pressure Level
TF	Transfer Function
WHO	World Health Organization

1 Introduction

The environment noise is increasing due to growth of application of machines in the industry and also in the home appliance. Therefore, it is desired to damp such noise. The conventional method to acoustic noise control uses passive damping techniques which attenuates the undesired noise with physical materials [1]. However the passive damping techniques have certain disadvantages, therefore in 1936 first time the active noise control (ANC) proposed by Lueg [2]. In last decades, the active damping technique developed and implemented further and nowadays ANC can be found in a variety of application fields, e.g., aircraft cabins, cars, headset and in industrial fields.
This thesis deals with a specific application of ANC. Therefore the first chapter gives a short introduction to noise, passive noise control, active noise control and secondary path estimation.

1.1 Noise

Acoustic noise is defined as a loud, disturbing or unpleasant sound, which is usually random or irregular. Sound is an energy which travels in form of waves through the air or through some other medium, we sense those waves with our ears and hear it. The human ear can hear acoustic sounds within the frequency range of 20 Hz to 20 kHz. Distinction between sound and vibration is based on their presence. Sound represents generally an audible phenomenon and vibration represents relatively the low frequency disturbances of solid structures, which we can sense through our body [4]. A vibrating surface can also generate a sound in the audible frequency range.
As depicted in Figure 1.1, the human ear reacts differently depending on a sound frequency and pressure level. The most sensitive frequency range is between 100 Hz and 8 kHz which is the range of human speech. The human ear is less sensitive for a sound with frequency under 100 Hz and above 18 kHz. The sound with high sound pressure level (SPL) could cause hearing impairments or damages.[5].

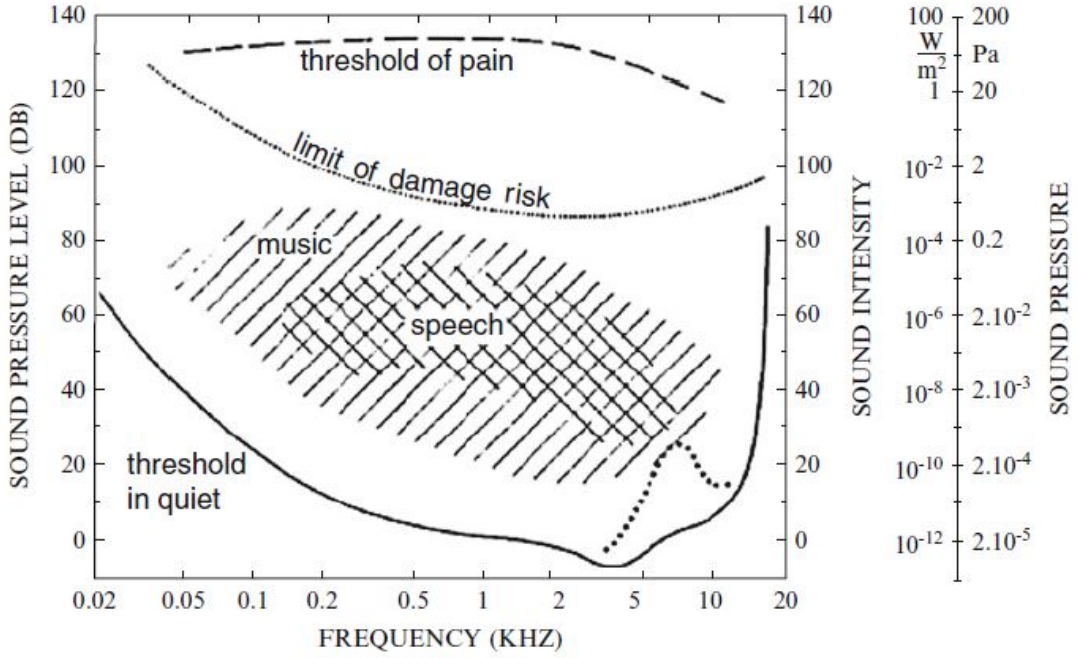

Figure 1.1: Human hearing range [3].

Two types of noise exist in the environment, broadband and narrowband. Broadband noise is random and it distributes its energy more or less evenly across the frequency band. Example of broadband noise is low frequency sounds of jet planes or impulse noise of explosion. Broadband signal used in different measurement and signal processing application as a test signal, which is called white and pink noise. Narrowband noise is periodic or nearly periodic signal and it concentrates its energy at small range of frequencies. This type of noise caused from rotating or repetitive machines. Example of narrowband noise is compressors in refrigerators, internal combustion engines used in transportation and as well as stationary applications [6].

1.2 Introduction to noise control

In order to control the noise it is important to understand, what is the noise source and how is the noise transmitted. Noise is transmitted from source to receiver by many different path, this can be generally grouped into airborne and structure-borne paths.

- Airborne path: the source radiates the sound through the surrounding air and then the sound is transmitted to the receiver. It can pass through some solid

partitions in between, e.g., walls, floors and ceilings.

- Structure-borne path: the source generates the mechanical vibration and this vibration is transmitted through the structure, which radiates a noise. This noise transmits through an airborne path to the receiver [4].

The conventional noise control is to use passive damping technique or to redesign the system. Despite that, the passive noise control is primarily effective for high frequency noise and redesigning the system is very costly. Generally noise above 1000 Hz is damped mostly by passive noise control method. Therefore active noise control methods are introduced to damp a noise in range between 50 Hz and 1000 Hz [7].

1.2.1 Passive noise control

In passive damping techniques, there are two distinct physical principles to control the sound transmission. These physical principles are the reflection and the dissipation principles.
Both the reflection and the dissipation principles are used for the airborne path transmitted noise. The reflection principle uses some solid partitions, enclosures and barriers to hinder the radiation of noise. However, using such enclosures and barriers for damping the noise is costly and the part adds also mass to the system. On the other hand, the dissipation methods use some absorptive treatments, which converts the sound energy to heat. Many passive noise control methods combine both principles, e.g., enclosures with absorptive linings, barriers with absorptive face and double skin partitions with an absorptive treatment between two skins.
The structure-borne noise transmission applies also both principles. The reflection principle based methods are impedance mismatch or vibration isolation and the dissipation principle employs some damping treatments. The following passive vibration control can be used to attenuate a noise, which is transmitted through a structure-borne path [4].

- Impedance mismatching: modify the design of structure to reduce the transfer of vibrational energy from the directly excited structure.

- Vibration isolation: add resilient elements between the structure that directly excited and other attached structures.

- Damping: apply highly dissipative materials to the vibrating structure and convert the vibration to the heat. Damping can be also improved by connecting ancillary structures to reduce the friction or by attaching damped resonators.
- Structural modification: add some mass or change the stiffness to achieve different level of impedance or shift the resonance frequencies.
- Dynamic neutralizers: attach ancillary mechanical resonators to the structure. In a narrow frequency region apply strong dynamic reaction forces to reduce the vibrational response of connected structures.

As above stated passive noise controls are very efficient for primary high frequency noise. However, passive techniques add weight on the system or changes the structure, this could lead to other problems, e.g., cost increment and redesign of whole system.

1.2.2 Active noise control

ANC represents an electro-acoustic or an electromechanical system that cancels undesired noise based on the principle of superposition. ANC creates antinoise with an equal amplitude and an opposite phase of source noise, this antinoise is referred to as a secondary source. At the end, the source noise and the secondary source both must compensate. Since characteristics of the noise and environment are time varying, the undesired noises frequency, amplitude and phase are also non-stationary. Therefore the ANC may be adaptive.
An adaptive system often consists of a digital filter and an adaptation algorithm. The adaptive filter performs the signal processing and the adaptation algorithm adjusts the filter coefficients. A block diagram of general adaptive filter is depicted in figure 1.2, where x is the input signal to the adaptive filter and the output signal of the filter referred as y. To achieve the desired signal, the coefficients of the filter must adapt itself and change the values every time when there is new input signal given. This process is done by an adaptation algorithm. Subtraction between the output signal y and the desired signal d is an error signal e, which are the input parameter for the adaptation algorithm. The adaptation algorithm tries to minimize the error based on the input signal x [8].
The filter itself can be realized as (transversal) finite impulse response (FIR), (recursive) infinite impulse response (IIR), lattice or transform-domain filters. The most ordinary adaptive filter is the transversal filter, which uses least mean square (LMS) algorithm

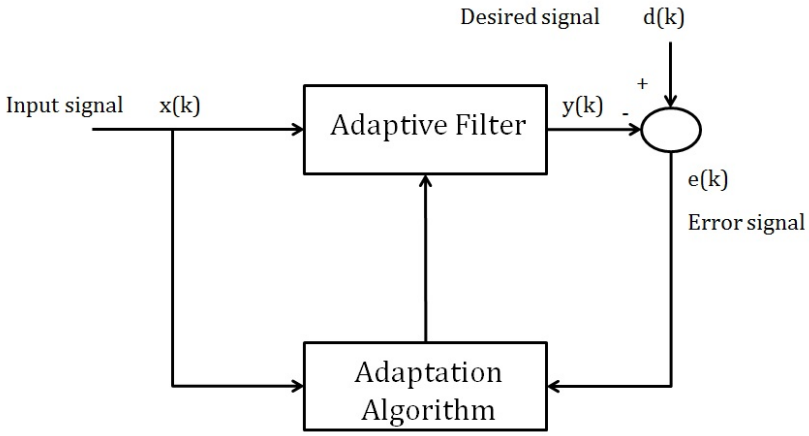

Figure 1.2: Adaptive System.

for minimizing error[1]. As introduced in section 1.1 there exist two types of noise in environment, broadband and narrowband. Their noise characteristics are distinctive from each other, hence different ANC systems are applied.

A broadband noise cancellation uses a reference input signal, which must correlate with the source noise. This source noise is referred as a primary noise. The reference input signal is mostly measured signal from microphone or sensor. The primary noise get canceled by a secondary source, the output of ANC. A narrowband noise cancellation uses information of the primary noise instead of measuring the reference input signal. Depending on the primary noise information, ANC generates the output signal and tries to cancel the known system frequencies and their harmonics.

ANC may have two different structures, feedforward and feedback control. The feedforward control uses FIR filter as an adaptive filter therefore it is referred as a feedforward control. The IIR filter is used as an adaptive filter for the feedback control and therefore it is referred as a feedback control.

The Feedforward control inserts the reference input signal to the controller before it propagates to the secondary source, based on this input signal controller attempts to compensate the primary noise. The residue of cancellation is measured by error sensor and this error signal is fed back to the ANC as an input signal.On the other hand, the feedback control tries to cancel primary noise without the reference input signal, it has only the error input signal. The Feedforward control is more robust than the feedback control, in case the reference input signal good isolated from the secondary source. The broadband and the narrowband noises can be eliminated by both control methods. However, in practice the feedforward method is used more than feedback control due to the control stability [9].

The broadband feedforward ANC consists of a reference input signal, a secondary source and an error input signal. The reference and the error input signals measured mainly by a microphone or a sensor. The secondary source is the canceling source and in the most cases speakers are used. One type of broadband noise is duct noise from exhaust pipes or ventilation systems. The feedforward control system of duct noise is depicted in Figure 1.3.

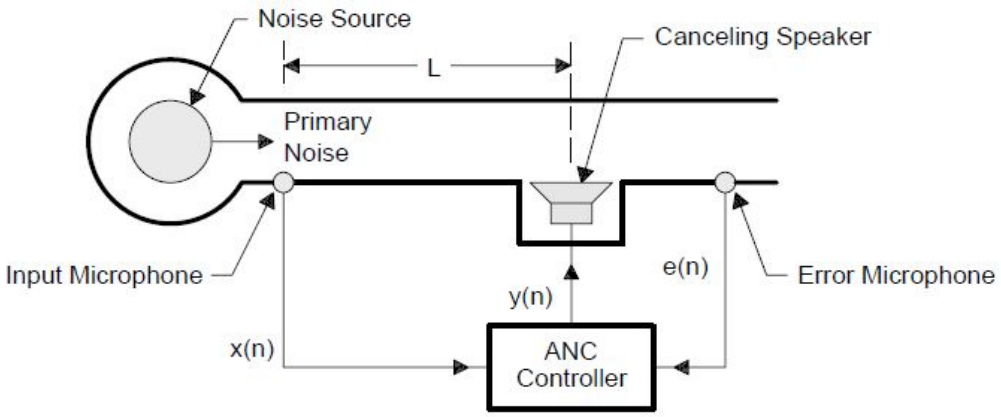

Figure 1.3: Single-Channel Broadband Feedforward ANC System in a Duct [6].

In this ANC, the input microphone used as a reference input signal and the error microphone measures the cancellation residue. A canceling speaker used as a secondary source. To satisfy the stability and causality of ANC, the reference input signal must be measured early enough that, by the time the primary source reaches the canceling speaker, an antinoise signal can be generated. In case the primary noise is a harmonic signal, then the antinoise signal must have same amplitude as the primary noise and 180 degree phase shifted. After cancellation process, the error microphone measures the residue signal and feedback this value to adaptive filter. The filter coefficients adapt itself for minimization of the error.
In case the primary noise is narrowband noise, the reference input signal can be nonacoustic signal such as value from tachometer, accelerometer or optic sensor. Therefore, the narrowband feedforward ANC consists of a reference input sensor, an error input microphone and a secondary source. Since the reference input signal is nonacoustic signal, there will be no feedback between the secondary source and the reference input signal. Single-channel narrowband ANC system depicted in Figure 1.4.
Based on reference sensor value, controller decides what kind of signal to generate. This generated signal must be synchronous by the time primary noise reach the canceling

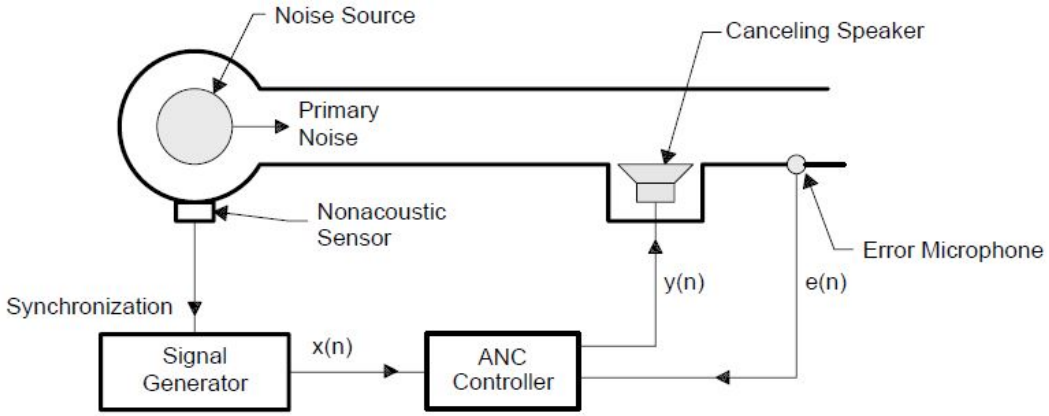

Figure 1.4: Single-Channel Narrowband Feedforward ANC System [6].

speaker position. The speaker tries cancel the main frequency and the harmonics of the primary noise. As same as in broadband feedforward ANC, the error microphone measures the noise residue and feedback to the controller.

Feedback ANC consists of only an error input signal and a secondary source. Based on the error input signal, ANC generates the secondary source. This noise controller proposed by Olson and May in 1953 [10]. The feedback ANC delivers limited attenuation over restricted frequency range for periodic or band limited noise. However, this method can be applied to the narrowband noise control due to known frequencies of the noise. The feedback ANC system is depicted in Figure 1.5. The narrowband feedforward ANC control can be also combined with feedback ANC for predicting the reference input signal [6].

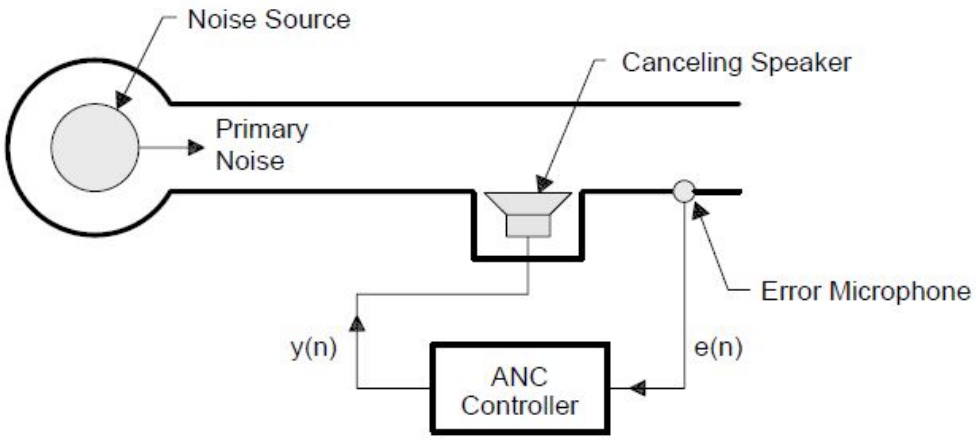

Figure 1.5: Single-Channel Feedback ANC System [6].

1.3 Introduction to secondary path

In section 1.2 the working principle of ANC is described. Based on this theoretical introduction to ANC, the secondary path is now introduced. All ANC have at least a secondary source and an error sensor. The error sensor measures the residue noise, which is combination of the primary noise and the secondary source. The secondary source signal influences to the error signal and this influence can lead to wrong system adaption. Therefore, it is necessary to identify and to compensate a secondary path transfer function S(z), which is path between the secondary source and the error sensor. In case the ANC is designed as Figure 1.3, then the secondary path may include digital-to-analog converter (DAC) , reconstruction filter, power amplifier, canceling speaker, acoustic path from canceling speaker to error microphone, preamplifier, anti aliasing filter and analog-to-digital converter (ADC) [9].

The secondary path can be estimated offline during the system is in a standstill. In the offline estimation, the ANC sends a test signal to the speaker and the system output signal gets measured with an error microphone as depicted in Figure 1.6. Using this test signal and measured signal, the secondary path can be estimated by different methods such as Least Mean Square (LMS) or other parameter identification algorithms. Otherwise, ANC can estimate the path online during system operation. The parameter identification algorithm can be also used for online path estimation.

The estimated path $\hat{S}(z)$ can be applied in two ways [11]. The first way is to place the inverse filter, $S(z)^{-1}$ in series with $S(z)$, which means the output signal need to be filtered additionally with $S(z)^{-1}$. The other way is to filter the reference input signal with $\hat{S}(z)$ before adding to the adaptive filter.

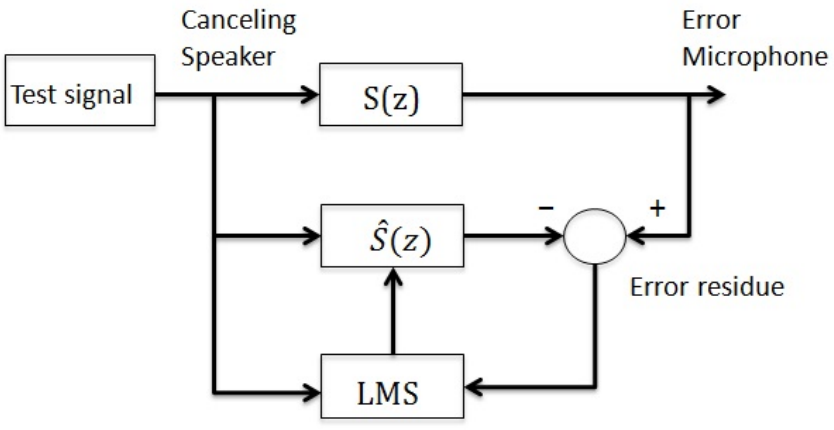

Figure 1.6: Secondary Path estimation with LMS Algorithm.

1.4 Motivation and Problem Statement

The company LOGICDATA is middle size global company and the head quarter is located in Deutschlandsberg, Austria. The Products of company divide into two distinct areas, the Business Units LOGIC OFFICE and LOGIC HOME. The Business Unit LOGIC HOME are mechatronic products for the home furniture industry. The Business Unit LOGIC OFFICE are electronic and mechatronic components for height adjustable sit-stand working places in the office furniture industry.
The main product of the LOGIC OFFICE Unit is a height adjustable desk. This height adjustable desk in most case consists of two drives, a control box, a handset and a desk plate. The desk can driven to the desired position in a limited range by pressing a button on the handset and the handset sends the command to the control box. The control box moves the drives to the desired position.
The height adjustable desk provides better working condition for the desk-based workers. The only disadvantage of this product is the drive noise during movement. The drives as depicted in Figure 1.7, vibrate with wide range of frequency and this vibration transferred to the desk plate. The desk plate converts the vibration to noise. The main noise sources of the system are the drives and rack of drives.

Figure 1.7: SLIMdrive 660s drive [12].

The World Health Organization(WHO) defines the desired maximum SPL of the workspace at office 55 dB and industry 85 dB. The maximum allowed SPL is 90 dB at workspace, in case it exceeds the limit, the noise could cause in the long run some diseases, e.g., hearing loss, cardiovascular risks and hypertension [13]. Since in most offices people share the room with other colleagues, the maximum SPL can reach from time to time. Studies also showed that people work more productive and can concentrate longer in less noisy environment [14]. To improve better working environment, the reduction of drive noise is necessary. To eliminate the noise by using passive noise control would be costly and also desk drives not in continuous movement. Therefore the motivation of this thesis is to damp the vibration and noise level of adjustable desk by active noise control.

1.5 Organization of this Work

This thesis is organized in two main parts as depicted in 1.8. The first part covers introduction to noise control, theory of methods, which are used for the secondary path estimation and theory of the used active noise control algorithm. This part consists of Chapter 1, 2 and 3. Chapter 1 gives brief introduction about noise and vibration, a passive and an active noise control methods,and a secondary path. In the second chapter presents the theory of the adaptive LMS algorithm for FIR filter, the recursive and not recursive LMS algorithm for IIR filter. A Filtered-x LMS (FxLMS) algorithm is used as an ANC algorithm and FxLMS is described in Chapter 3. The second part of the thesis, covers the experimental set up of system and result of ANC. In the chapter 4, the components are used in the experiment are introduced. In the sections 4.2 and 4.3, two experimental set-ups are described and results of ANC are shown. Finally, the outcome of this thesis will be summarized in the conclusion and the further steps are described in the outlook.

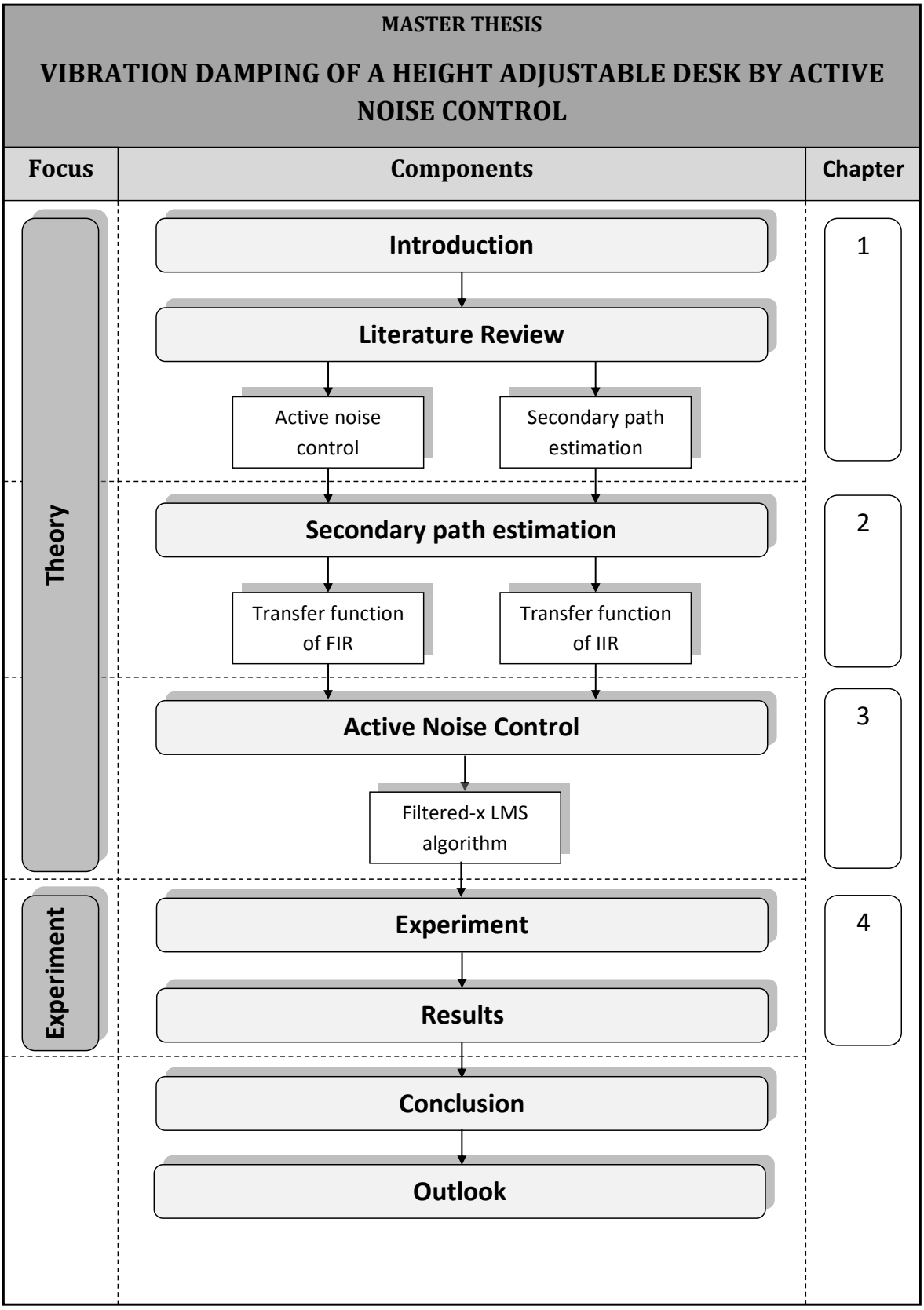

Figure 1.8: Structure of the Master Thesis.

2

Secondary Path Estimation

A secondary path is estimated in this thesis with two different approach. The first approach is an adaptive LMS algorithm based on FIR filter, which estimates the path offline. Second method is a LMS algorithm based on IIR filter, which estimates the path offline and also recursively online. In this chapter, the theory of both methods will be presented.

2.1 Adaptive LMS Algorithm for FIR Filter

The Least Mean Square algorithm is one of most widely used algorithm in adaptive filter [15]. An FIR filter is used as an adaptive filter in the adaptive LMS algorithm. The adaptive FIR filter consists of three basic parts, a unit delay element, adder and multiplier as depicted in Figure 2.1. Since the FIR filter is a feedforward filter, the number of delay elements determine the finite duration of its impulse response and the filter order. The FIR filter with order $N-1$ has N number of filter coefficients $b_i(k)$, where $i = 0, 1, \cdots, N-1$, which also referred to as weights $w_i(k)$. The filter coefficients multiplied with delayed input data sequence $\{x(k) \quad x(k-1) \quad \cdots \quad x(k-N+1)\}$, which is the output signal and it can be expressed as

$$y(k) = \sum_{i=0}^{N-1} w_i(k)x(k-i) \tag{2.1}$$

If the input vector at time k defined as

$$\mathbf{x}(k) = \begin{bmatrix} x(k) & x(k-1) & \cdots & x(k-N+1) \end{bmatrix}^T \tag{2.2}$$

where T denotes transpose of matrix and the weight vector at time k as

$$\mathbf{w}(k) = \begin{bmatrix} w_0(k) & w_1(k) & \cdots & w_{N-1}(k) \end{bmatrix}^T \tag{2.3}$$

then, the output signal $y(k)$ can be expressed as

$$y(k) = \mathbf{w}^T(k)\mathbf{x}(k) \tag{2.4}$$

This equation is called a finite convolution sum, because it convolves the finite duration impulse response of the filter $\mathbf{w}$(k) with filter input x(k) to generate the filter output y(k).

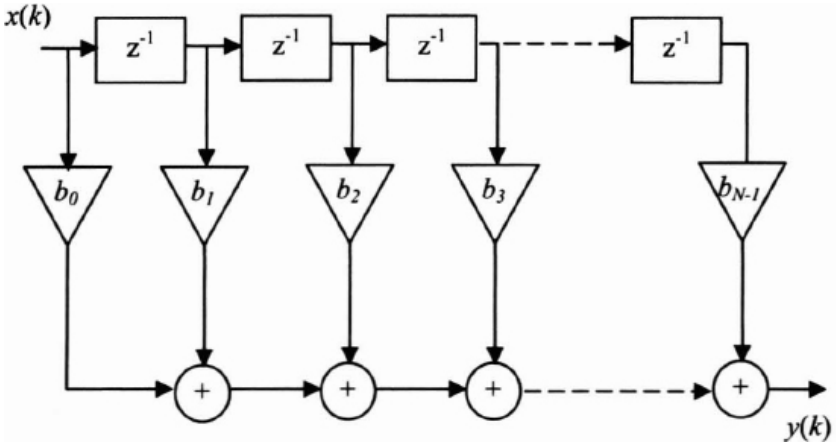

Figure 2.1: Finite Impulse Response (FIR) Filter [16].

The output of the FIR filter is the output of the adaptive LMS algorithm. Therefore, the system output $y(k)$ is compared with the desired signal $d(k)$ as depicted in figure 1.2, which delivers the residue error $e(k)$ signal

$$\begin{aligned} e(k) &= d(k) - y(k) \\ &= d(k) - \mathbf{w}^T(k)\mathbf{x}(k) \end{aligned} \tag{2.5}$$

In order to determine the weight vector which decreases the error signal, the input and desired signal of system are assumed as statistically stationary [17].

2.1.1 Mean-Square Error

A mean-square of error signal $e(k)$ is minimized to find the weight vector $\mathbf{w}(k)$. The square of the error signal at time k is given by

$$\begin{aligned} e^2(k) &= (d(k) - \mathbf{w}^T(k)\mathbf{x}(k))(d(k) - \mathbf{x}^T(k)\mathbf{w}(k)) \\ &= d^2(k) + \mathbf{w}^T(k)\mathbf{x}(k)\mathbf{x}^T(k)\mathbf{w}(k) - 2d(k)\mathbf{x}^T(k)\mathbf{w}(k) \end{aligned} \tag{2.6}$$

An expected value of the mean-square of the error signal is referred as a Mean-Square Error (MSE) and the MSE of (2.6) can be expressed as

$$\begin{aligned} \xi(w) &= E[e(k)^2] \\ &= E[d(k)^2] + \mathbf{w}^T(k)E[\mathbf{x}(k)\mathbf{x}^T(k)]\mathbf{w}(k) - 2E[d(k)\mathbf{x}^T(k)]\mathbf{w}(k) \end{aligned} \tag{2.7}$$

where E denotes the statistical expectation operator. To simplify the above equation, an auto-correlation matrix of the input signal at time k is defined as

$$\begin{aligned} \mathbf{R} &= E[\mathbf{x}(k)\mathbf{x}^T(k)] \\ &= \begin{bmatrix} r_{xx}(0) & r_{xx}(1) & \cdots & r_{xx}(N-1) \\ r_{xx}(1) & r_{xx}(0) & \cdots & r_{xx}(N-2) \\ \vdots & \vdots & \ddots & \vdots \\ r_{xx}(N-1) & r_{xx}(N-2) & \cdots & r_{xx}(0) \end{bmatrix} \end{aligned} \tag{2.8}$$

where

$$r_{xx}(i) = E[x(k)x(k-i)] \tag{2.9}$$

and a cross-correlation vector between desired and input signals is defined as

$$\begin{aligned} \mathbf{p} &= E[d(k)\mathbf{x}(k)] \\ &= \begin{bmatrix} r_{dx}(0) & r_{dx}(1) & \cdots & r_{dx}(N-1) \end{bmatrix} \end{aligned} \tag{2.10}$$

where

$$r_{dx}(i) = E[d(k)x(k-i)] \tag{2.11}$$

Equations (2.8) and (2.10) are applied to (2.7) and

$$\begin{aligned}\xi(w) &= E[e(k)^2] \\ &= E[d(k)^2] + \mathbf{w}^T(k)\mathbf{R}\mathbf{w}(k) - 2\mathbf{p}^T\mathbf{w}(k)\end{aligned} \tag{2.12}$$

is the general performance function of a causal FIR adaptive filter with given weights. The MSE is a function of filter coefficients $\mathbf{w}(k)$ as shown in equation 2.12. For each value of the filter coefficient of $\mathbf{w}(k)$, there is corresponding scalar value of the MSE. Therefore, the MSE values associated with $\mathbf{w}(k)$ form an $(N+1)$ dimensional space, which is called as a MSE surface or a performance surface.

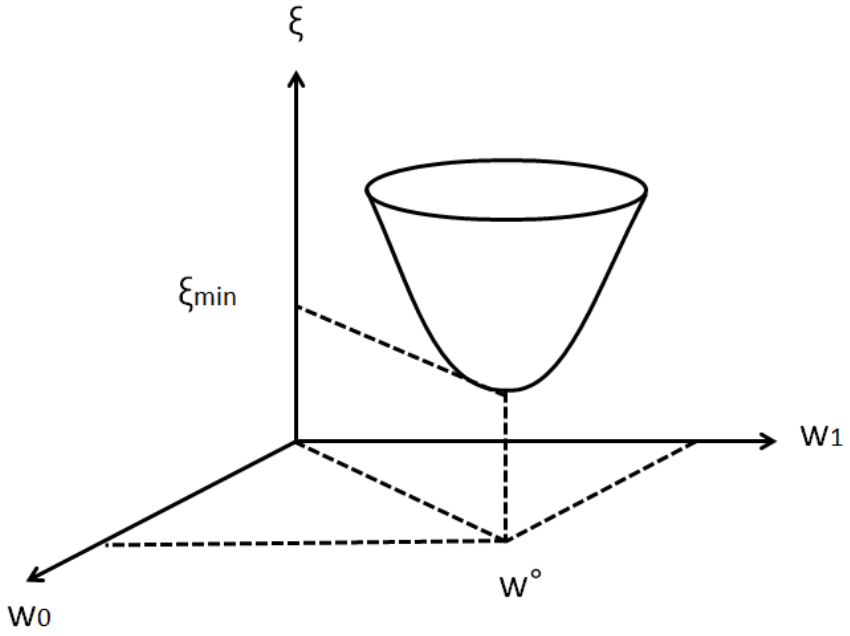

Figure 2.2: Three dimensional MSE surface, N = 2 case [9].

In case the filter order $N = 2$, then MSE surface is three dimensional as depicted in figure 2.2, where $\mathbf{w}^\circ = [w_0^\circ \quad w_1^\circ]$ is the filter coefficient vector and ξ_{min} is the expectation value of the minimum mean square error.The height of $\xi(k)$ corresponds to the power of error signal $e(k)$ and in case the filter coefficients change then the power of the error signal will also change.
The error surface is quadratic thus there exists an unique filter coefficient vector $\mathbf{w}(k) = \mathbf{w}^\circ$ which gives the minimum ξ_{min}. The optimal filter $\mathbf{w}^\circ$ can be applied to equation (2.12) as follows

$$\mathbf{R}\mathbf{w}^\circ = \mathbf{p} \tag{2.13}$$

$$\xi_{min} = E[d^2(k)] - \mathbf{p}^T\mathbf{w}^\circ. \tag{2.14}$$

If the above equation is combined with equations (2.12) and (2.13), then the general MSE equation can be expressed as

$$\begin{aligned}\xi(k) &= \xi_{min} + [\mathbf{w}(k) - \mathbf{w}^\circ]^T\mathbf{R}[\mathbf{w}(k) - \mathbf{w}^\circ] \\ &= \xi_{min} + \mathbf{v}^T(k)\mathbf{R}\mathbf{v}(k)\end{aligned} \tag{2.15}$$

where

$$\mathbf{v}(k) = \mathbf{w}(k) - \mathbf{w}^\circ \tag{2.16}$$

is the weight misalignment vector, which is the difference between the adaptive filter coefficients and optimal solution. The error surface is concave and there exists one unique minimum. To reach the bottom of convex, the unique minimum, we need an algorithm which search the minimum automatically from error surface. There are various gradient-based algorithms available and one of them is a method of steepest descent.

2.1.2 Method of Steepest Descent

The steepest descent method is an iterative technique which is suitable to derive adaptive algorithm since the related error surface is guaranteed to be quadratic with respect to filter weights $\mathbf{w}(k)$. Geometrically, it is possible to reach the minimum with the adaptation of the filter weights in the direction of the steepest descent on the convex error surface.

The method of steepest descent moves on the error surface in the direction of a weighted negative gradient. The filter weights are updated at each iteration in the direction of the negative gradient of the error surface [9]. If $\xi(0)$ is the value of the MSE at time $k = 0$ with an arbitrary choice of the weight vector $\mathbf{w}(0)$. At any point on the surface $[\mathbf{w}(0), \xi(0)]$, the slope can be calculated by directional derivatives $\partial\xi(n)/\partial w_i$. The gradient of the surface $\nabla\xi(k)$ is defined as the vector of the directional derivatives. The steepest descent algorithm is implemented as follows

$$\mathbf{w}(k+1) = \mathbf{w}(k) - \frac{\mu}{2}\nabla\xi(k) \tag{2.17}$$

where μ is the step size, which controls the rate of descent. The larger the value of μ is, the faster the speed of descent. The step size μ can be selected in the range of

$$0 < \mu < \frac{2}{NP_x} \tag{2.18}$$

where N is the filter order and P_x is the input signal power, which is calculated as

$$P_x = r_{xx}(0) = E[x^2(k)]. \tag{2.19}$$

Since μ is dependent from filter order N, the small μ is used for large order filters. On the other hand μ is also inversely proportional to the input signal power. This means the weaker signals can use larger μ and the stronger signals have to use smaller μ.
The vector $\nabla\xi(k)$ denotes the gradient of the function with respect to $\mathbf{w}(k)$ and the negative sign increments the adaptive weight vector in the negative gradient direction. The error gradient from equation (2.12) can be calculated as following

$$\nabla\xi(k) = -2\mathbf{p} + 2\mathbf{R}\mathbf{w}(k). \tag{2.20}$$

From above two equations, the final form of steepest descent algorithm can be derived as

$$\mathbf{w}(k+1) = \mathbf{w}(k) + \mu[\mathbf{p} - \mathbf{R}\mathbf{w}(k)]. \tag{2.21}$$

The weight vector $\mathbf{w}(k)$ converges to $\mathbf{w}^\circ$ this means it reaches the minimum point of the error surface, where the gradient is zero, $\nabla\xi(k) = 0$.

2.1.3 LMS Algorithm

The statistical properties of the input signal $x(n)$ and the desired signal $d(n)$ are unknown in most of the practical applications. Therefore, the method of steepest descent must be modified. The estimated MSE is the squared error sample

$$\hat{\xi}(k) = e^2(k). \tag{2.22}$$

The estimated gradient is the gradient of the single squared error sample

$$\nabla\hat{\xi}(k) = 2[\nabla e(k)]e(k). \tag{2.23}$$

The error signal from the equation (2.5) is replaced to above equation, then the gradient of error sample look as following

$$\nabla e(k) = -\mathbf{x}(k) \tag{2.24}$$

and the estimated gradient becomes

$$\nabla \hat{\xi}(k) = -2\mathbf{x}(k)e(k). \tag{2.25}$$

Finally, the adaptive LMS algorithm or stochastic gradient algorithm is defined as at time k

$$\mathbf{w}(k+1) = \mathbf{w}(k) + \mu\mathbf{x}(k)e(k). \tag{2.26}$$

The block diagram of LMS algorithm with adaptive FIR filter in discrete time domain is shown in figure 2.3.

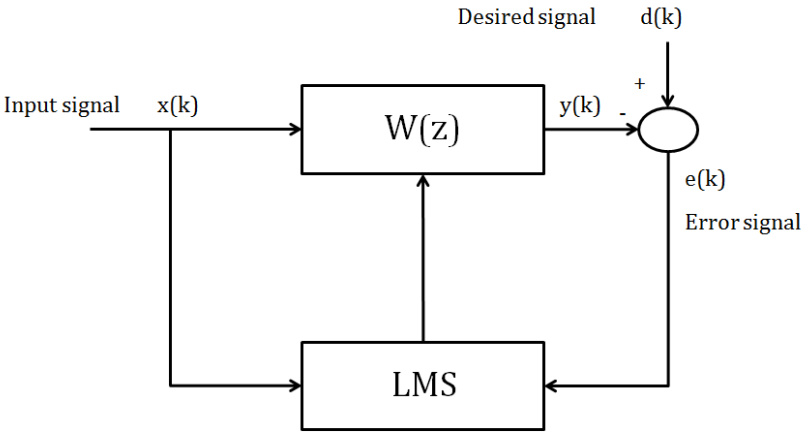

Figure 2.3: Adaptive LMS Algorithm

To summarize, there are four steps to perform the adaptive LMS algorithm for FIR filter:

1. Choose parameters and initial conditions: N, μ and $\mathbf{w}(0)$, where N is the filter order, μ is the step size, and $\mathbf{w}(0)$ is the initial weight vector at time $k = 0$.

2. Compute adaptive filter output:

$$y(k) = \sum_{i=0}^{N-1} w_i(k)x(k-i) \tag{2.27}$$

3. Compute error signal:

$$e(k) = d(k) - y(k) \tag{2.28}$$

4. Update the adaptive filter coefficients using the LMS algorithm:

$$w_i(k+1) = w_i(k) + \mu x(k-i)e(k), \quad i = 0, 1, \cdots, N-1 \tag{2.29}$$

2.2 LMS Algorithm for IIR Filter

The second method to estimate the secondary path, is a LMS algorithm based on an IIR filter [18] and [19]. The LMS algorithm for IIR filter can estimate the secondary path either offline or recursively online. In the next sections both methods are described. Generally LMS algorithm for IIR filter requires a test input signal and a corresponding output signal of system. The test input signal has to be long enough, that the system response can be identified. Based on this two signal, the transfer function is estimated. IIR filter can achieve same performance as an FIR filter, but with lower filter order. IIR filters with an order, that is sufficient high, can match poles and zeros of physical systems, where FIR filter can only approximate it. However, IIR filter has a feedforward and a feedback loop. The impulse response of IIR filter is illustrated in the figure 2.4 and its transfer function is given by

$$H(z) = \frac{B(z)}{A(z)} = \frac{b_0 + b_1 z^{-1} + \cdots + b_n z^{-n}}{1 + a_1 z^{-1} + \cdots + a_n z^{-n}} \tag{2.30}$$

where $[b_0 \quad b_1 \quad \cdots \quad b_n]$ are the numerator coefficients of the IIR filter, or the feedforward loop coefficients. The feedback loop coefficients are $[1 \quad a_1 \quad \cdots \quad a_n]$, which is also the denominator coefficients of IIR filter. The filter coefficients can be merged to one λ matrix as

$$\lambda^T = \begin{bmatrix} a_1 & \cdots & a_n & b_0 \cdots & b_n \end{bmatrix} \tag{2.31}$$

where λ^T is $(2n+1)$ sized vector.

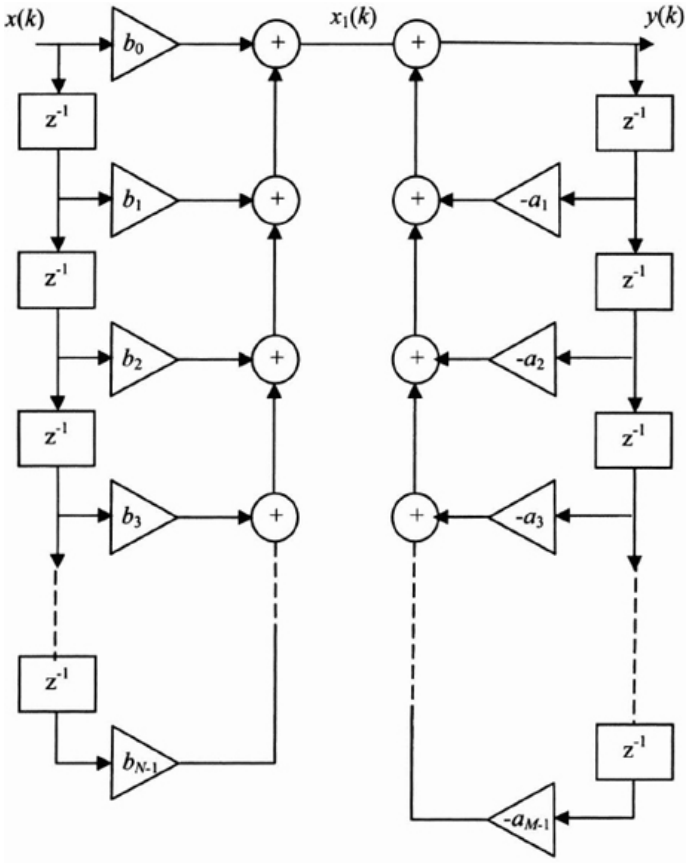

Figure 2.4: Infinite Impulse Response (IIR) Filter [16].

2.2.1 LMS Algorithm for IIR Filter

The LMS Algorithm for IIR Filter estimates the path between the input signal and the output signal of system. The real path is referred to as $H(z)$ and estimated path is denoted as $\hat{H}(z)$

$$\hat{H}(z) = \frac{\hat{B}(z)}{\hat{A}(z)} = \frac{\hat{b}_0 + \hat{b}_1 z^{-1} + \cdots + \hat{b}_n z^{-n}}{1 + \hat{a}_1 z^{-1} + \cdots + \hat{a}_n z^{-n}} \tag{2.32}$$

where $[\hat{b}_0 \quad \hat{b}_1 \quad \cdots \quad \hat{b}_n]$ and $[1 \quad \hat{a}_1 \quad \cdots \quad \hat{a}_n]$ are estimated filter coefficients. The filter coefficients matrix $\hat{\lambda}$ is denoted as follows

$$\hat{\lambda}^T = \begin{bmatrix} \hat{a}_1 & \cdots & \hat{a}_n & \hat{b}_0 \cdots & \hat{b}_n \end{bmatrix} \tag{2.33}$$

The block diagram of the LMS algorithm with IIR filter is illustrated in figure 2.5.

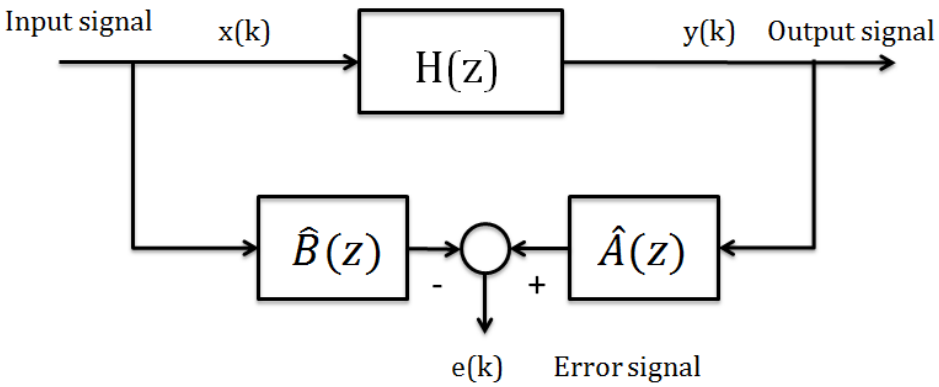

Figure 2.5: LMS Algorithm for IIR Filter.

As depicted in the figure 2.5, the error signal can be calculated as

$$\begin{aligned} e(z) &= \hat{A}(z)y(z) - \hat{B}(z)x(z) \\ &= y(k) + \hat{a}_1 y(k-1) + \cdots + \hat{a}_n y(k-n) - (\hat{b}_0 x(k) + \hat{b}_1 x(k-1) + \cdots + \hat{b}_n x(k-n)) \end{aligned} \tag{2.34}$$

The goal of the LMS algorithm is to fulfill $\lambda = \hat{\lambda}$, which means the error value should approximate to zero. Therefore, the mean-square error (MSE) method can be also used here as in adaptive LMS algorithm. The sum of squared errors

$$e^2(n) + e^2(n+1) + \cdots + e^2(L) \tag{2.35}$$

where n is the filter order and L is the input signal length. The error value is calculated for each sample as below

$$\begin{aligned} e(n) &= y(n) + \hat{a}_1 y(n-1) + \cdots + \hat{a}_n y(0) - (\hat{b}_0 x(n) + \hat{b}_1 x(n-1) + \cdots + \hat{b}_n x(0)) \\ e(n+1) &= y(n+1) + \hat{a}_1 y(n) + \cdots + \hat{a}_n y(1) - (\hat{b}_0 x(n+1) + \hat{b}_1 x(n) + \cdots + \hat{b}_n x(1)) \\ &\vdots \\ e(L) &= y(L) + \hat{a}_1 y(L-1) + \cdots + \hat{a}_n y(L-n) - (\hat{b}_0 x(L) + \hat{b}_1 x(L-1) + \cdots \\ &\quad + \hat{b}_n x(L-n)). \end{aligned} \tag{2.36}$$

If we formulate the above equations in vector form, the error signal vector is

$$\mathbf{e} := \begin{bmatrix} e(n) \\ e(n+1) \\ \vdots \\ e(L) \end{bmatrix} \tag{2.37}$$

and the output vector is

$$\mathbf{y} := \begin{bmatrix} y(n) \\ y(n+1) \\ \vdots \\ y(L) \end{bmatrix} \tag{2.38}$$

and the matrix of the input and output signals is defined as $\mathbf{M}$

$$\mathbf{M} := \begin{bmatrix} -y(n-1) & \cdots & -y(0) & u(n) & \cdots & u(0) \\ -y(n) & \cdots & -y(1) & u(n+1) & \cdots & u(1) \\ \vdots & & \vdots & \vdots & & \vdots \\ -y(L-1) & \cdots & -y(L-n) & u(L) & \cdots & u(L-n) \end{bmatrix} \tag{2.39}$$

where the M matrix has dimension$(L-n+1) \times (2n+1)$. Equation (2.36) can be expressed as

$$\mathbf{e} = \mathbf{y} - \mathbf{M}\hat{\boldsymbol{\lambda}}. \tag{2.40}$$

The sum of squared error can be written as follows

$$\begin{aligned} \xi &= \mathbf{e}^T\mathbf{e} \\ &= e^2(n) + e^2(n+1) + \cdots + e^2(N) \\ &= (\mathbf{y} - \mathbf{M}\hat{\boldsymbol{\lambda}})^T(\mathbf{y} - \mathbf{M}\hat{\boldsymbol{\lambda}}) \\ &= (\mathbf{y}^T - \mathbf{M}^T\hat{\boldsymbol{\lambda}}^T)(\mathbf{y} - \mathbf{M}\hat{\boldsymbol{\lambda}}) \\ &= \mathbf{y}^T\mathbf{y} + \hat{\boldsymbol{\lambda}}^T\mathbf{M}^T\mathbf{M}\hat{\boldsymbol{\lambda}} - \mathbf{y}^T\mathbf{M}\hat{\boldsymbol{\lambda}} - \hat{\boldsymbol{\lambda}}^T\mathbf{M}^T\mathbf{y} \\ &= \mathbf{y}^T\mathbf{y} + \hat{\boldsymbol{\lambda}}^T\mathbf{M}^T\mathbf{M}\hat{\boldsymbol{\lambda}} - 2\mathbf{y}^T\mathbf{M}\hat{\boldsymbol{\lambda}}^T. \end{aligned} \tag{2.41}$$

To achieve the optimal solution, the gradient of ξ must be equal to zero

$$\frac{\partial \xi}{\partial \hat{\lambda}} = 0. \tag{2.42}$$

If the equation (2.42) is applied to equation (2.41), then it will look as follows

$$\begin{aligned} \frac{\partial \xi}{\partial \hat{\lambda}} &= 2(\mathbf{M}^T\mathbf{M})\hat{\boldsymbol{\lambda}} - 2(\mathbf{y}^T\mathbf{M})^T \\ &= 2[(\mathbf{M}^T\mathbf{M})\hat{\boldsymbol{\lambda}} - (\mathbf{M}^T\mathbf{y})] = 0 \end{aligned} \tag{2.43}$$

and

$$(\mathbf{M}^T\mathbf{M})\hat{\boldsymbol{\lambda}} - (\mathbf{M}^T\mathbf{y}) = 0. \tag{2.44}$$

If the $\mathbf{M}^T\mathbf{M}$ is regular then $\hat{\boldsymbol{\lambda}}$ can be calculated as

$$\hat{\boldsymbol{\lambda}} = (\mathbf{M}^T\mathbf{M})^{-1}\mathbf{M}^T\mathbf{y}. \tag{2.45}$$

For the path estimation, a suitable test signal for the identification is sent to the system and the output signal is measured. With this output $\mathbf{y}$ and test or input signal $\mathbf{x}$, M can be found. After that, the coefficient of the secondary path can be estimated using equation 2.45. The LMS algorithm for IIR filter can be also extended as recursive LMS algorithm as shown in the next section.

2.2.2 Recursive LMS Algorithm for IIR Filter

If the system changes its characteristics during run time, online estimation methods are needed. The recursive LMS algorithm for IIR filter estimates the secondary path online, when each time the system receives new measured input and output values. Based on this two values, matrix $\mathbf{M}$ and output signal $\mathbf{y}$ are updated and new $\hat{\boldsymbol{\lambda}}$ vector is calculated. For each new sample, the new values are calculated and added to the bottom of matrices and vectors.
If IIR filter has order n and the signal length L, then $\mathbf{M}_N$ and $\mathbf{y}_N$ matrices will look

$$\mathbf{M}_L = \begin{bmatrix} -y(n-1) & \cdots & -y(0) & u(n) & \cdots & u(0) \\ -y(n) & \cdots & -y(1) & u(n+1) & \cdots & u(1) \\ \vdots & & \vdots & \vdots & & \vdots \\ -y(L-1) & \cdots & -y(L-n) & u(L) & \cdots & u(L-n) \end{bmatrix} \tag{2.46}$$

and

$$\mathbf{y}_L = \begin{bmatrix} y(n) \\ y(n+1) \\ \vdots \\ y(L) \end{bmatrix}. \tag{2.47}$$

If the system received new input and output values, then $\mathbf{M}_{N+1}$ and $\mathbf{y}_{N+1}$ matrices will be updated as follows

$$\begin{aligned} \mathbf{M}_{L+1} &= \begin{bmatrix} -y(n-1) & \cdots & -y(0) & u(n) & \cdots & u(0) \\ -y(n) & \cdots & -y(1) & u(n+1) & \cdots & u(1) \\ \vdots & & \vdots & \vdots & & \vdots \\ -y(L-1) & \cdots & -y(L-n) & u(L) & \cdots & u(L-n) \\ -y(L) & \cdots & -y(L-n+1) & u(L+1) & \cdots & u(L-n+1) \end{bmatrix} \\ &= \begin{bmatrix} \mathbf{M}_L \\ \mathbf{m}_{L+1}^T \end{bmatrix} \end{aligned} \tag{2.48}$$

where

$$\mathbf{m}_{L+1}^T = \begin{bmatrix} -y(L) & \cdots & -y(L-n+1) & u(L+1) & \cdots & u(L-n+1) \end{bmatrix} \tag{2.49}$$

and

$$\mathbf{y}_{L+1} = \begin{bmatrix} \mathbf{y}_L \\ y_{L+1} \end{bmatrix}. \tag{2.50}$$

The matrix $\hat{\boldsymbol{\lambda}}_{L+1}$ can be calculated as

$$\begin{aligned} \hat{\boldsymbol{\lambda}}_{N+1} &= \left(\begin{bmatrix} \mathbf{M}_L \\ \mathbf{m}_{L+1}^T \end{bmatrix}_T \begin{bmatrix} \mathbf{M}_L \\ \mathbf{m}_{L+1}^T \end{bmatrix} \right)_{-1} \begin{bmatrix} \mathbf{M}_L \\ \mathbf{m}_{L+1}^T \end{bmatrix}_T \begin{bmatrix} \mathbf{y}_L \\ y_{L+1} \end{bmatrix} \\ &= \left(\begin{bmatrix} \mathbf{M}_L^T & \mathbf{m}_{L+1} \end{bmatrix} \begin{bmatrix} \mathbf{M}_L \\ \mathbf{m}_{L+1}^T \end{bmatrix} \right)^{-1} \begin{bmatrix} \mathbf{M}_L^T & \mathbf{m}_{L+1} \end{bmatrix} \begin{bmatrix} \mathbf{y}_L \\ y_{L+1} \end{bmatrix} \\ &= (\mathbf{M}_L^T \mathbf{M}_L + \mathbf{m}_{L+1} \mathbf{m}_{L+1}^T)^{-1} (\mathbf{M}_L^T \mathbf{y}_L + \mathbf{m}_{L+1} y_{L+1}) \end{aligned} \tag{2.51}$$

To simplify the calculation, the above equation is split into smaller equation. At the end, we will get following final equations for recursive LMS algorithm for IIR filter

$$\mathbf{m}_{L+1}^T = \begin{bmatrix} -y_L & \cdots & -y_{L-n+1} & u_{L+1} & \cdots & u_{L-n+1} \end{bmatrix} \tag{2.52}$$

$$\mathbf{k}_{L+1} = \frac{\mathbf{P}_L \mathbf{m}_{L+1}}{1 + \mathbf{m}_{L+1}^T \mathbf{P}_L \mathbf{m}_{L+1}} \tag{2.53}$$

$$\hat{\boldsymbol{\lambda}}_{L+1} = \hat{\boldsymbol{\lambda}}_L + \mathbf{k}_{L+1}(y_{L+1} - \mathbf{m}_{L+1}^T \hat{\boldsymbol{\lambda}}_L) \tag{2.54}$$

$$\mathbf{P}_{L+1} = \mathbf{P}_L - \mathbf{k}_{L+1} \mathbf{m}_{L+1}^T \mathbf{P}_L \tag{2.55}$$

where $\hat{\boldsymbol{\lambda}}_L$ and $\mathbf{P}_L := (\mathbf{M}_L^T \mathbf{M}_L)^{-1}$ are known from previous calculation.

3

Active Noise Control

Active noise control is chosen based on which type of a noise or a vibration need to be canceled. The ANC basic methods are introduced in section 1.2.2. Since the vibration of a height adjustable desk is a broadband signal in a frequency range up to 8 kHz, a broadband feedforward active noise control is preferred. One of the most commonly used and easy to implement broadband feedforward ANC is the Filtered-x LMS (FxLMS) algorithm [9]. Therefore, the FxLMS algorithm is used as ANC and it is introduced in the next section.

3.1 Filtered-x LMS Algorithm

The FxLMS algorithm is a modified form of an adaptive LMS algorithm for FIR filters, which has additionally a secondary path [9]. The block diagram of the ANC system using the FxLMS algorithm is depicted in figure 3.1. In this figure, outside of the dashed line block represents the acoustic domain and the system paths between sensors and sources. $P(z)$ is a primary path, which is the path between the input reference sensor and the error sensor. $S(z)$ is a secondary path, which is the path between the secondary source and the error sensor. Inside of the dashed line block represents the FxLMS algorithm, where $\hat{S}(z)$ is the estimated secondary path as referred to chapter 2 and $W(z)$ is the FIR filter of the adaptive LMS algorithm.
The estimated secondary path $\hat{S}(z)$ is applied to the measured reference sensor signal x and this filtered reference sensor signal x' is used as an input signal in the adaptive LMS algorithm [20]. The adaptive LMS algorithm adapts the filter coefficients of $W(z)$ to minimize the error residue of the ANC and the output of the algorithm is denoted as y. The output signal y travels to the error sensor position, which means the y is filtered with the secondary path $S(z)$ and this signal is denoted as y'. The primary noise at the position of the error sensor is named as desired signal d. The summing junction represents the vibration damping process, where the canceling signal y' meets

the desired signal d. The subtraction of this two signals is the error residue of the ANC, which is measured by the error sensor e.

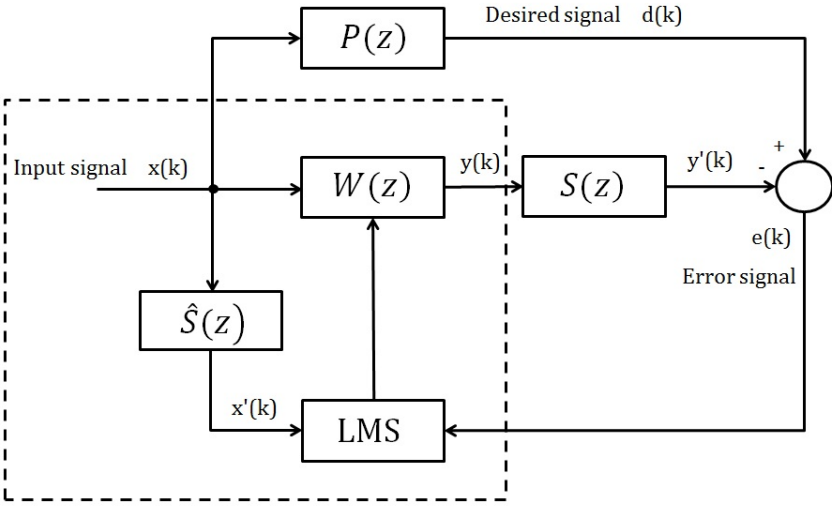

Figure 3.1: Block diagram of FxLMS algorithm.

The FxLMS algorithm can be expressed in the same way as the adaptive LMS algorithm presented in section 2.1 except of choice of the input signal $\mathbf{x}(k)$. The input signal $\mathbf{x}(k)$ has to be filtered with the estimated secondary path $\hat{S}(z)$ before it enters the adaptive LMS algorithm. The estimated secondary path can be applied to input signal $\mathbf{x}(k)$ and denoted as $\mathbf{x}'(k)$

$$\mathbf{x}'(k) = \hat{\mathbf{s}}(k) * \mathbf{x}(k) \tag{3.1}$$

where k is the time index, $\hat{s}(k)$ is the impulse response of the estimated secondary path $\hat{S}(z)$, and $*$ denotes the linear convolution.
If the estimated secondary path $\hat{S}(z)$ is represented by a FIR filter with M elements such that

$$\hat{\mathbf{s}}(k) = \begin{bmatrix} \hat{s}_0(k) & \hat{s}_1(k) & \cdots & \hat{s}_{M-1}(k) \end{bmatrix}^T \tag{3.2}$$

then $\mathbf{x}'(k)$ can be expressed as

$$\mathbf{x}'(k) = \begin{bmatrix} \sum_{i=0}^{M-1} \hat{s}_i(k)x(k-i) \\ \sum_{i=0}^{M-1} \hat{s}_i(k)x(k-i-1) \\ \vdots \\ \sum_{i=0}^{M-1} \hat{s}_i(k)x(k-i-N+1) \end{bmatrix}. \tag{3.3}$$

The FIR filter of the FxLMS algorithm is calculated as follows

$$\mathbf{w}_i(k+1) = \mathbf{w}_i(k) + \mu\mathbf{x}'(k)e(k). \tag{3.4}$$

In the FxLMS algorithm, the maximum step size μ_{max} can be estimated approximately [21] by

$$\mu_{max} = \frac{1}{P_{\mathbf{x}'}(N + \triangle)} \tag{3.5}$$

where $P_{\mathbf{x}'}$ is the power of the filtered input signal $\mathbf{x}'$, N is the FIR filter order, and $\triangle$ is the number of samples, which correspond to the delay between the secondary source and the error sensor.
To summarize, there are five steps to perform the FxLMS algorithm:

1. Estimate the secondary path $\hat{S}(z)$ either offline only once or recursively online for each iteration.

2. Choose parameters and initial conditions: N, μ and $\mathbf{w}(0)$, where N is the filter order, μ is the step size, and $\mathbf{w}(0)$ is the initial weight vector at time $k = 0$.

3. Compute FIR filter output with measured input signal:

$$y(k) = \sum_{i=0}^{N-1} w_i(k)x(k-i) \tag{3.6}$$

4. Apply the secondary path to the input signal x:

$$\mathbf{x}'(k) = \begin{bmatrix} \sum_{i=0}^{M-1} \hat{s}_i(k)x(k-i) \\ \sum_{i=0}^{M-1} \hat{s}_i(k)x(k-i-1) \\ \vdots \\ \sum_{i=0}^{M-1} \hat{s}_i(k)x(k-i-N+1) \end{bmatrix} \tag{3.7}$$

5. Update the FIR filter coefficients with the measured error signal:

$$w_i(k+1) = w_i(k) + \mu x'(k-i)e(k), \quad i = 0, 1, \cdots, N-1 \tag{3.8}$$

Detail related to the algorithm can be found in [9].

4 Experiment

Vibration damping experiments are performed for two different set-ups. For the each set-up the secondary path is estimated and FxLMS algorithm applied as an ANC. First, the ANC is tested with different single sinusoidal signals. Then, the ANC tested with measured signal from a height adjustable desk.
In the first section of the chapter, the components for the experimental set-ups are introduced. In the next two sections, the experimental set-ups are described, and results of the secondary path identification and the FxLMS algorithm are shown for each set-up.

4.1 Components

Before measurements and tests are performed on a height adjustable desk, it was desired to verify the algorithms and also the components in an experimental set-up, which has as less as possible influence from the surrounding environment. Therefore, the algorithms are tested and verified with an experimental set-up. The experiment components contain two vibro-speaker, which are used as a shaker, two acceleration sensor, DSP board as a digital control system, and a wooden plate. The experiment set-up is assembled on a vibration isolator table from Thorlabs [22] to achieve linear system and have no influence from surrounding environment.

4.1.1 Wooden plate

The wooden plate is made of chipboard, or is also called as a particle board. The size of the wooden plate is 74×89 cm and it is $25mm$ thick. A speed of sound in common wood is $4000m/s$ and the speed of sound in chipboard is approximately $3500m/s$ at a room temperature. This means, the plate will have a wave propagation delay up to $0.254ms$. This delay must be covered by the estimated secondary path.

4.1.2 Vibro-speaker

The two vibro-speakers are used as a shaker in the experiment. In figure 4.1 the vibro-speaker is shown. The first shaker excites the plate with a provided signal, that it is used as a primary source. The second shaker is used as a secondary source, which excites the plate with an anti noise signal. The shaker has a frequency range from $80Hz$ to $18kHz$ and has a root mean square (RMS) output power of $5W$ with DC 5V supply voltage.

Figure 4.1: Vibro-speaker from Adin [23].

4.1.3 Acceleration sensor

Two acceleration sensors are used from the company measurement specialties [24]. In figure 4.2 the accelerometer is shown. The ACH-01 is a piezoelectric accelerometer and it measures only in a z-axis direction. The supply drain voltage is from $3V$ to $40V$ and the sensitivity of the sensor is from $7mV/g$ to $11mV/g$ at a room temperature. The frequency range of the sensor is from $2Hz$ to $20kHz$. The measured signals from the sensors are amplified with gain factor 28, to achieve better signal noise ratio (SNR).

Figure 4.2: ACH-01 Accelerometer from Measurement specialties [24].

4.1.4 DSP board

A DSP Starter Kit (DSK) for the TMS320C6713 is used as a digital control system [25]. The TMS320C6713 DSK is made by Spectrum Digital Incorporated and it is a development platform for Texas Instruments floating point C6713 DSP. The DSK can be programmed and debugged with an interface, Code Composer Studio from Texas Instrument.

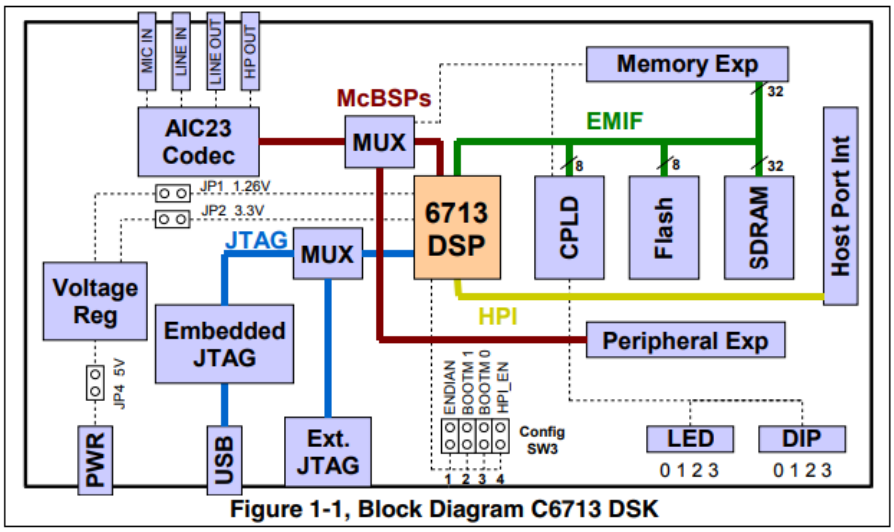

Figure 4.3: TMS320C6713 DSP Starter Kit from Spectrum Digital Incorporated [25].

As depicted in the figure 4.3, the C6713 DSK contains:

- A Texas Instrument TMS320C6713 floating point DSP operating at $225MHz$.
- A TLV320AIC23 stereo codec operating at $12MHz$ system clock and the supported sampling frequencies are from $8kHz$ to $96kHz$. The stereo codec provides a SNR Multibit Sigma-Delta $90dB$ ADC and $100dB$ DAC, which are weighted at $48kHz$ frequency. It has four $3.5mm$ audio jacks, microphone input, line input, line output, and headphone.
- $16Mbytes$ of synchronous DRAM.
- $512Kbytes$ of non-volatile Flash memory.
- Four user accessible LEDs and DIP switches.
- JTAG emulation through on-board JTAG emulator with USB host interface.

- Single voltage power supply $+5V$.

In the experiment, the two acceleration sensors are connected to codec line input's left and right channel. The secondary source shaker is connected to codec line output. The ADC receives the signals from the sensors and convert them to the discrete values to ADC counts. The ANC FxLMS algorithm runs at TMS320C6713 DSP on a real time and calculates the output value based on those discrete input values. After that, the output value of the FxLMS algorithm is sent to DAC and then the converted analog signal is transmitted to the secondary source shaker.

4.2 First Experimental Set-Up

The first experimental set-up is depicted in figure 4.4. As shown in the figure 4.4 the four edges of the wooden plate are mounted on the vibration isolator table from Thorlabs. Between the wooden plate and the vibration isolator table, a tension springs with $35mm$ height are mounted on the four edges, to isolate the wooden plate from the mounted bottom surface.

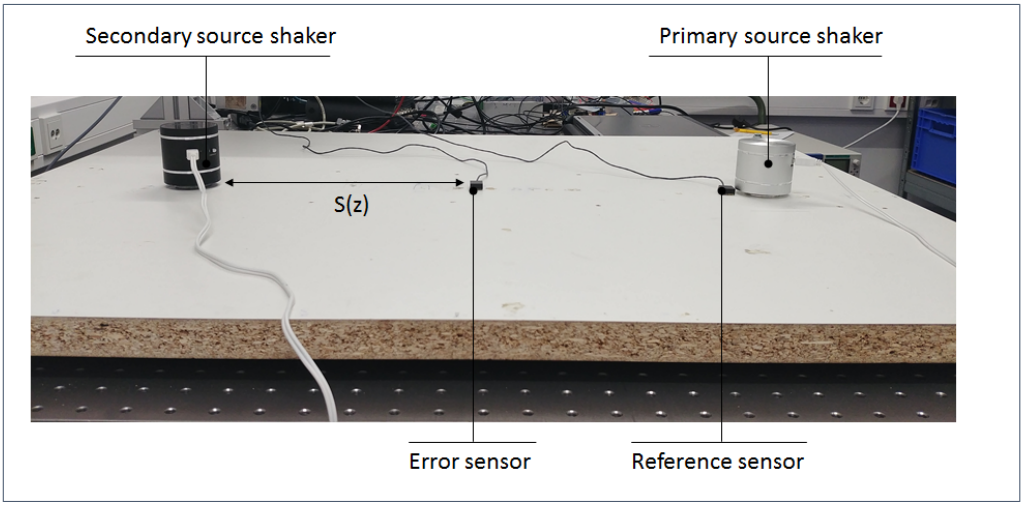

Figure 4.4: First experimental set-up

The silver vibro-speaker is used as a primary source shaker and the black vibro-speaker is used as a secondary source shaker. The sensor placed next to the silver vibro-speaker is the reference sensor and the sensor positioned in the middle of the plate is the error sensor.

For defining the position for the shakers and sensors, the wooden plate is excited with single $1kHz$ sinusoidal signal from the shakers and then the plate vibration is measured with the acceleration sensor in the different positions on the plate. The primary source shaker is placed on the right side of the plate, since in the real height adjustable desk, the drives are mounted in the middle of the left and right side of the desk plate. The secondary source shaker is positioned, where the highest signal amplitude is measured from the primary source shaker. The reference sensor has to be placed at the nearest possible to the primary source and as far as possible from the secondary source. If the reference sensor is placed near to the secondary source, then the system will have an unwanted feedback loop from the secondary source to the reference sensor, which may hinder the ANC. The error sensor position is defined, where the highest signal amplitude is measured from the both source shakers.

4.2.1 Secondary path estimation of first experimental set-up

As depicted in figure 4.4, the path between the secondary source shaker and the error sensor is the secondary path. This path will be estimated offline with the adaptive LMS algorithm for FIR filter and with the LMS algorithm for IIR filter.
To understand the system better, the vibration of the height adjustable desk is measured with acceleration sensor. The acceleration sensor was placed on the top of the height adjustable desk, where the drive was mounted on the other side. The vibration of the height adjustable desk is measured, while the height adjustable desk drives from upwards to downwards and also from downwards to upwards. The measurement result is evaluated with a Matlab and a Fast Fourier Transform (FFT) of the time signal is shown in figure 4.5.
As can be observed from the above figure, there are many signals with high amplitude in a frequency range up to $1kHz$ and then the signal amplitudes are similar in a frequency range from $1kHz$ to $8kHz$. The signals with a frequency above $8kHz$ do not have a big amplitude and therefore it is not interesting for the ANC.
Since the relevant signals are in a frequency range up to $8kHz$, the sampling rate $16kHz$ will be sufficient for the ANC and for the secondary path estimation.
Firstly, the secondary path of the wooden plate is estimated with chirp signal in a frequency range from $20Hz$ to $8KHz$. The adaptive LMS algorithm for FIR filter had a step size $\mu = 1^{-9}$ and filter order $N = 200$. The last calculated FIR filter coefficients are taken as estimated secondary path. The LMS algorithm for IIR filter had a filter order $N = 64$. The bode diagrams of the both estimated secondary paths are shown in

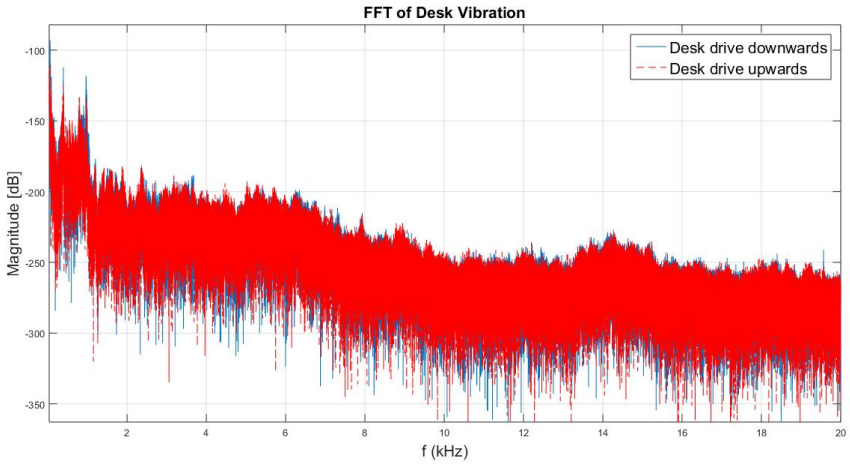

Figure 4.5: FFT of desk vibration in both direction.

figure 4.6. The amplitude of the signals are little bit different but in general the both bode diagram look similar to each other.

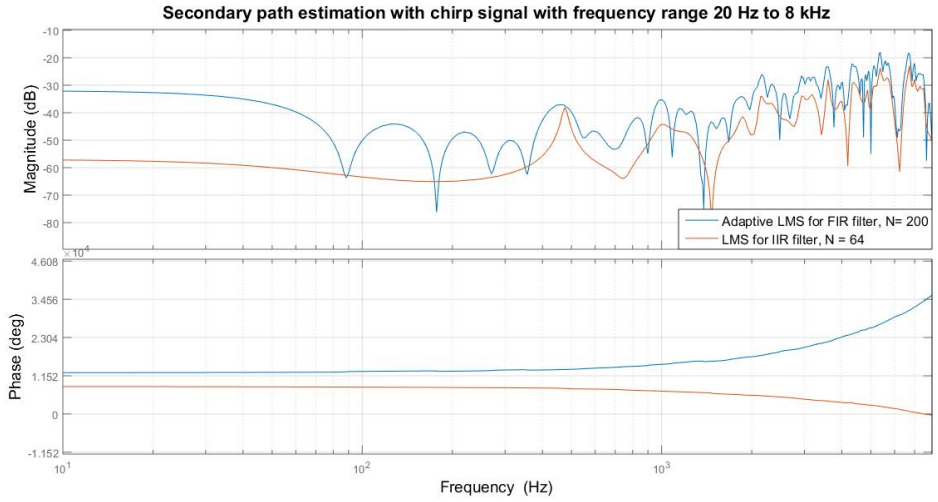

Figure 4.6: Bode diagram of estimated secondary path using adaptive LMS algorithm for FIR filter and LMS algorithm for IIR filter.

To verify the estimated paths, the paths are applied to the chirp signal and compared with the measured error sensor signal. The outcomes are depicted in figure 4.7. In the simulation results, the actual measured signal from the error sensor is referred as e and the estimated value from the secondary path as $\hat{e}$. If the secondary path is estimated correctly then the signals e and $\hat{e}$ should be identical. As shown in figure 4.7(b), the error residue of the estimation using the LMS algorithm for IIR filter is smaller than

the adaptive LMS algorithm. This means, that the estimation of the LMS algorithm for IIR filter is more accurate than the adaptive LMS for FIR filer.

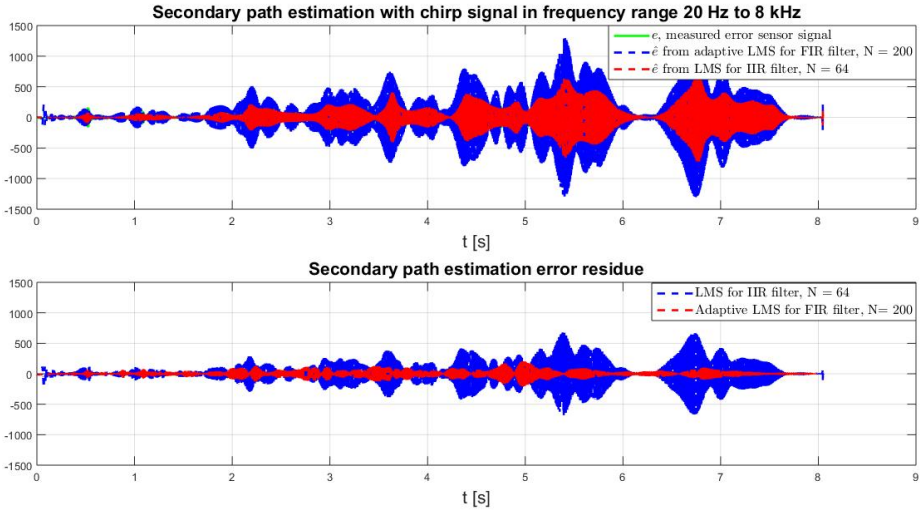

(a)

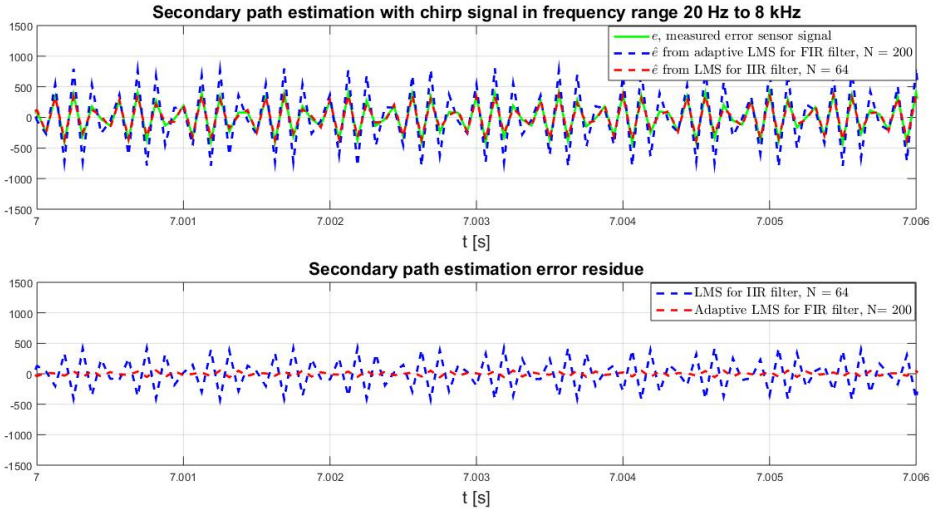

(b)

Figure 4.7: Secondary path estimated with chirp $20Hz$ to $8kHz$ signal. (a) Signal in a full range. (b) Signal in a short range for better visualization.

Secondly, the secondary path is estimated with white noise. Therefore the secondary path is also estimated with both algorithms and compared as above. The bode diagram of the estimated paths are depicted in figure 4.8. From the bode diagram can be seen the magnitude of the signals are similar the frequency under $3kHz$ and the frequency above $3kHz$ the magnitudes are the same. This shows that, the secondary paths are

estimated approximately correct.

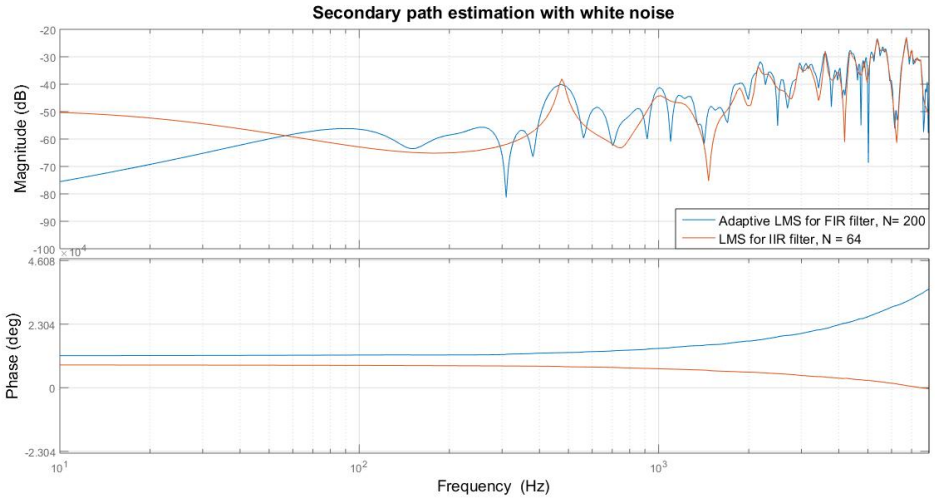

Figure 4.8: Bode diagram of estimated secondary path using adaptive LMS algorithm for FIR filter and LMS algorithm for IIR filter.

To verify the estimated paths, the paths are applied to the white noise and compared with the measured error sensor signal. The outcomes are depicted in the figure 4.9. From the simulation result, the error residue of the both estimations are smaller than the previous simulation with chirp signal. However, this time the error residue of adaptive LMS algorithm for FIR filter is smaller than the LMS algorithm for IIR filter. Overall, both secondary paths are good and can be used in FxLMS algorithm.
Since the implementation of a FIR filter is easier than the IIR filter, in the further steps the estimated secondary path from the adaptive LMS algorithm for FIR filter is used in the FxLMS algorithm. The estimated secondary path has a filter order $N = 200$ and the first 38 filter coefficients are near zero, which are caused from the delay between the error sensor and the secondary source shaker. The 38 samples means, the system has a $2.375ms$ delay for the sampling frequency $16kHz$.

4.2.2 ANC result of first experimental set-up

Firstly, the ANC FxLMS algorithm is tested with single sinusoidal signal with frequency $440Hz$ or $1kHz$ generated by the primary source shaker. The error and the reference sensors measure the vibration of the plate and based on measured sensors values, the FxLMS algorithm tries to damp the vibration at the position, where the error sensor is placed. The results of the experiment is shown in figure 4.10.

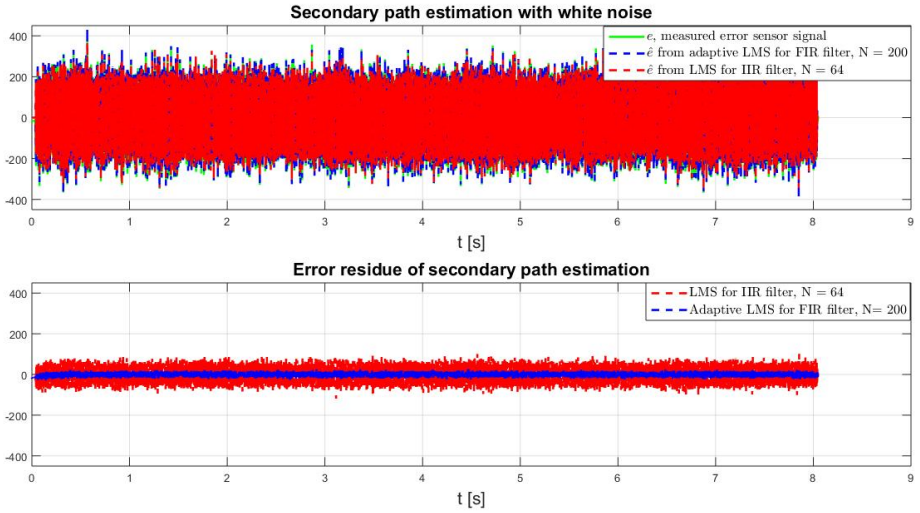

(a)

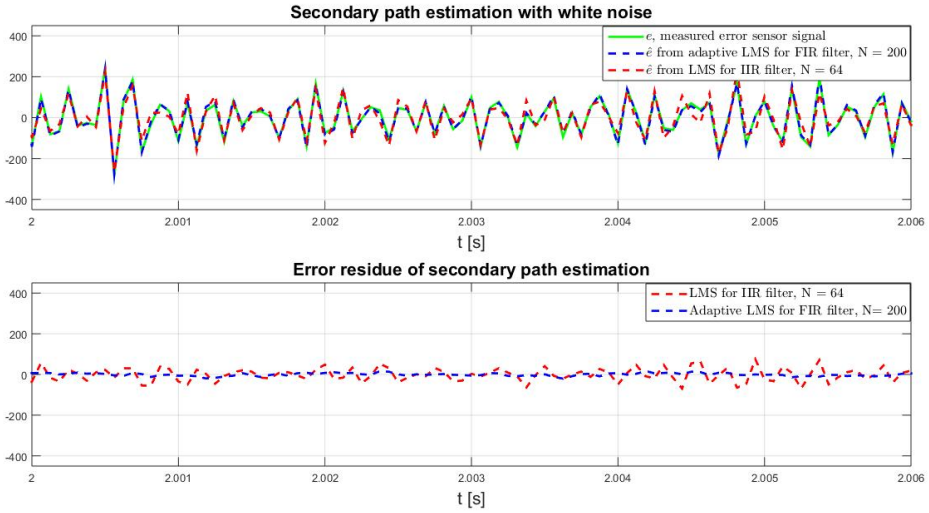

(b)

Figure 4.9: Secondary path estimated with white noise signal. (a) Signal in a full range. (b) Signal in a short range for better visualization.

In the figure, the blue signal is the output of FxLMS algorithm, which is the canceling signal. The green signal is the input signal, which is measured by reference sensor. The red signal is the error signal, which is measured by error sensor. The goal of this measurement is the error sensor signal goes to zero or to near zero. As shown in the figure 4.10(a), the ANC works for the both sinusoidal signals. In $440Hz$ sinusoidal signal, the amplitude of the error sensor signal is reduced from 200 to around 30 ADC counts within $80ms$. The $1kHz$ sinusoidal signal is achieved even better result and

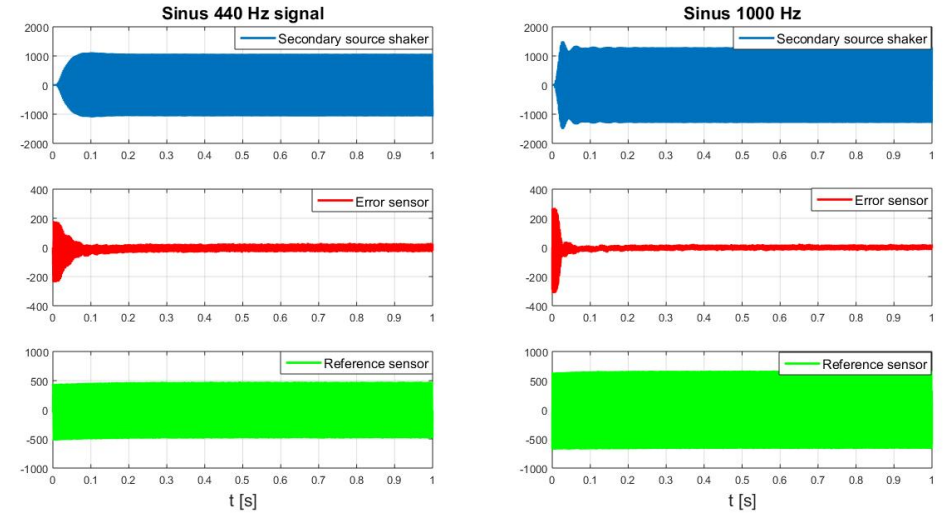

(a)

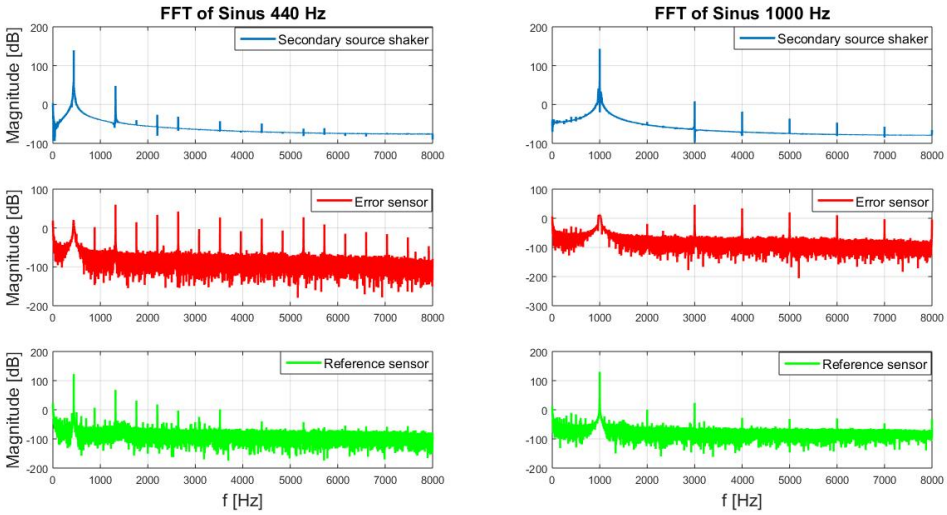

(b)

Figure 4.10: ANC of single sinusoidal signal using FxLMS algorithm. (a) In time domain. (b) In frequency domain.

the amplitude of the error sensor signal is reduced from 280 to around 20 ADC counts within $50ms$. Additional to that, the ANC was canceling some of the harmonics of the sinusoidal signal as shown in the figure 4.10(b).

However, the vibration was only damped partially, where the error sensor is placed, due to the radiation of the shaker on the plate is not a same everywhere. Even though the vibration was damped in the position of the error sensor, in some other positions, e.g. on the plate edges, the vibration was increasing. Therefore additionally, a sound

pressure level is measured with microphone in different positions and heights from the plate.
In the experiment, a $1kHz$ single sinusoidal signal is used and the FxLMS algorithm is applied. The microphone was placed on the middle of the plate and $100cm$ high from the plate. In this position, the SPL is increased approximately 17dB after ANC activation. After that, the microphone is placed on the edge of the plate and $15cm$ high from the plate and there the SPL is decreased approximately by $9dB$. The measurement from the microphone and the sensor are shown in figure 4.11, where figure 4.11(a) is the SPL increased and in the figure 4.11(b) is the SPL decreased.
Lastly, the FxLMS algorithm is tested with a signal, which is measured from a height adjustable desk. The desk signal is broadband signal as showed in the figure 4.5. The result is depicted in figure 4.12. From the figure 4.12(a) can be seen, the ANC did not work as expected. The amplitude of the FxLMS algorithm output signal is getting higher and tries to damp the vibration. The amplitude of the error sensor signal is decreased a little bit, but not as much as a single sinusoidal signal. However, the ANC damped the error sensor signal in some frequency range up to $12dB$ as shown in the figure 4.12(b).
Since in this experimental set-up, the ANC is strongly dependent from the position of the sensors and shakers, the experimental set-up is changed.

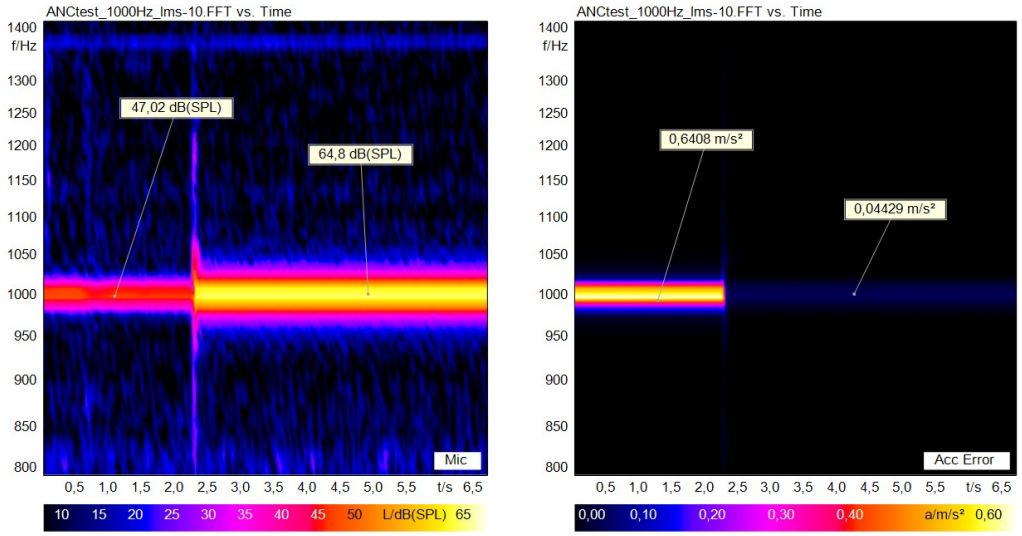

(a)

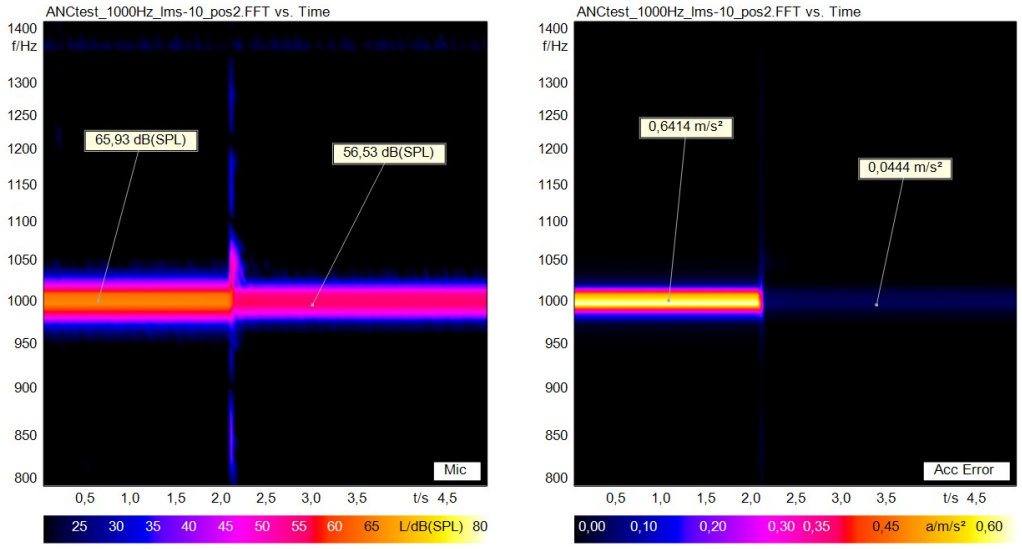

(b)

Figure 4.11: Microphone and error sensor measurement of $1kHz$ sinusoidal signal before and after ANC. (a) Microphone is positioned on the center of the plate, $100cm$. (b) Microphone is positioned on the side of the plate, $15cm$.

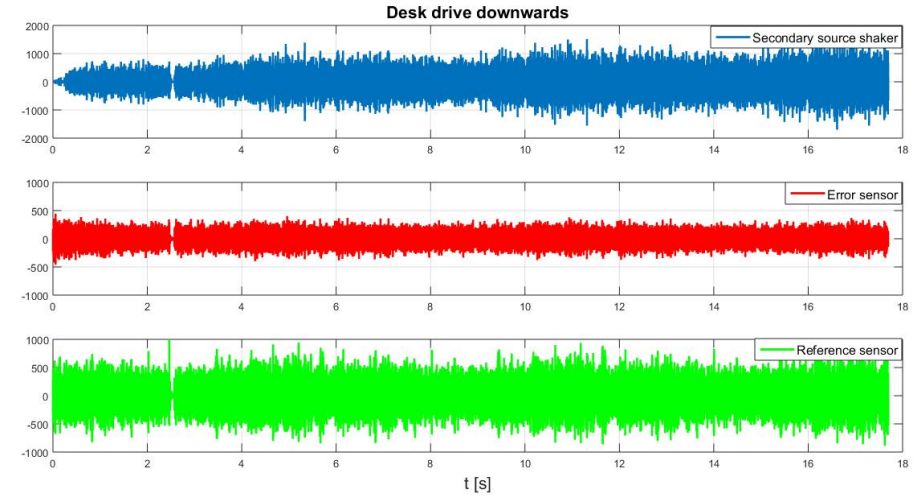

(a)

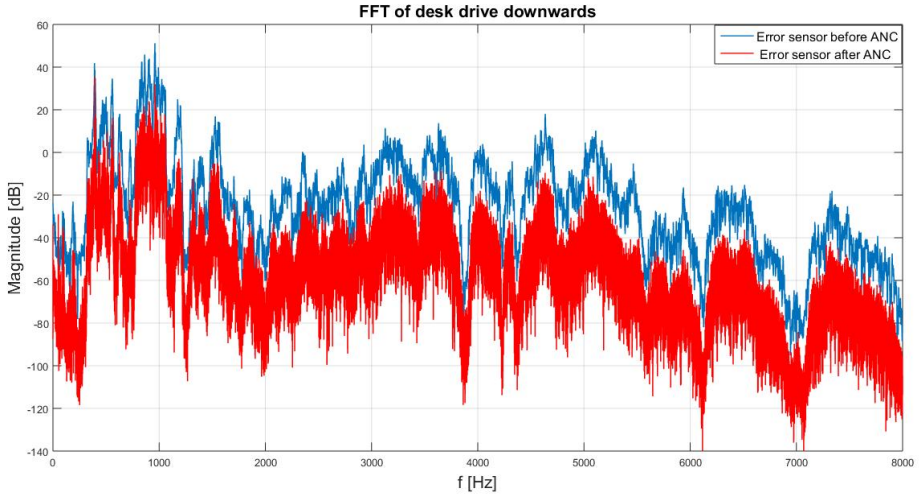

(b)

Figure 4.12: ANC of desk drive down signal using FxLMS algorithm. (a) In time domain. (b) In frequency domain.

4.3 Second Experimental Set-Up

For the second experimental set-up, the plate is mounted in the middle to the vibration isolator table in 40cm height. Since in the height adjustable desk, the drives are mounted each on left and right side of the desk, the second set-up will have similar behavior like the real system. The second experimental set-up is shown in the figure 4.13. The plate need to be excited from the bottom like the drives of the desk. Therefore the silver shaker is super glued on the bottom of the plate as a primary source. The opposite of the plate the black shaker is placed as a secondary source. The reference sensor is mounted on top of the silver shaker as shown in figure 4.13. The error shaker is positioned on top of the plate in 18cm from the front edge and in 44.5cm from the right edge.

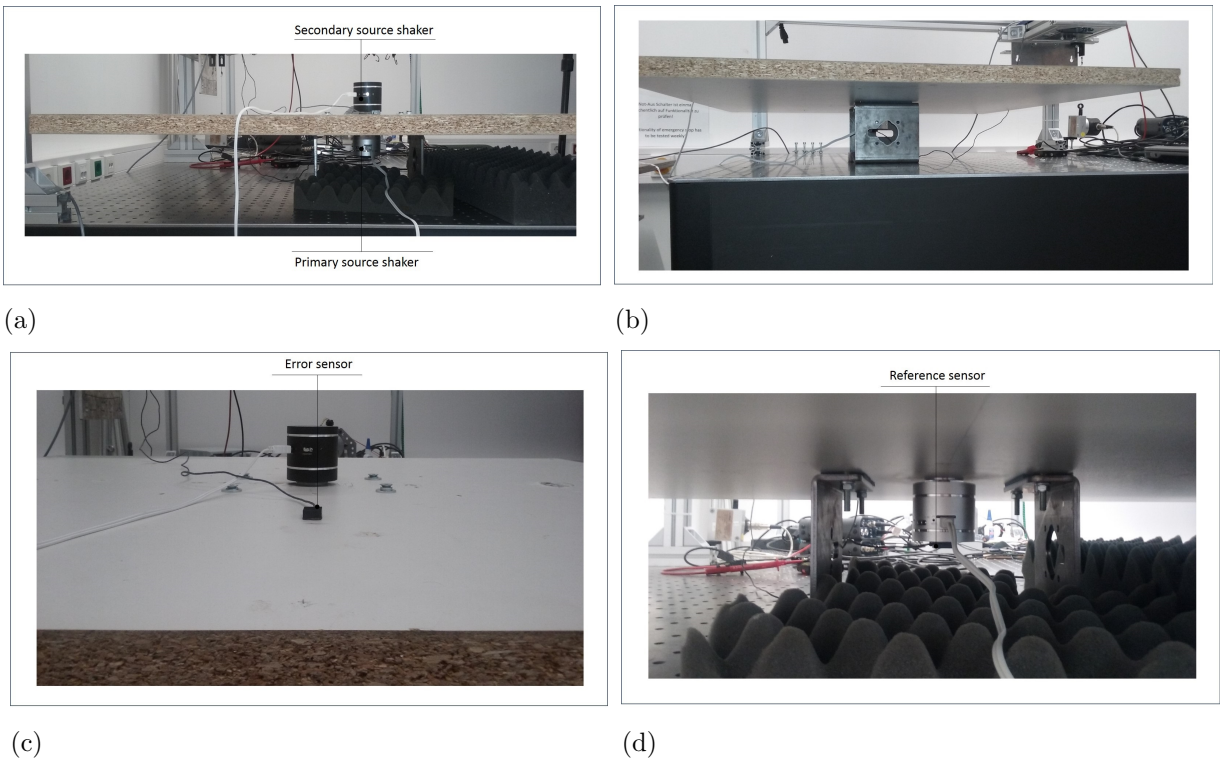

Figure 4.13: Second experimental set-up. (a) Front side. (b) Right side. (c) Top. (d) Bottom.

Since the both shaker placed exactly in the middle of the plate, the radiation of the vibration will be same on the plate except on the edges. Therefore, for defining the position of the error sensor, only the secondary source shaker was excited with 1kHz sinusoidal signal and selected the position, where the most amplitude is measured excluding the edges of the plate. After defining the optimal position for the sensors and

shakers, the secondary path estimation is performed with a white noise signal.

4.3.1 Secondary path estimation of second experimental set-up

The secondary path is estimated with the white noise signal using the adaptive FxLMS algorithm for FIR filter and the LMS algorithm for IIR filter. The algorithms have same parameters as in previous section 4.2.1. The adaptive FxLMS algorithm has a step size $\mu = 1^{-10}$ and a FIR filter order $N = 200$. The LMS algorithm has a IIR filter order $N = 64$. The bode diagram of the estimated secondary paths are shown in the figure 4.14.

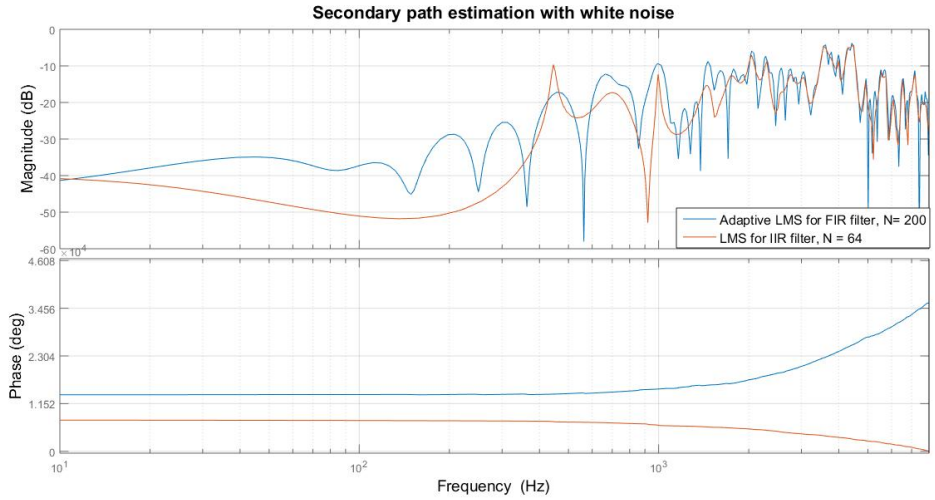

Figure 4.14: Bode diagram of estimated secondary path using adaptive LMS algorithm for FIR filter and LMS algorithm for IIR filter.

To verify the estimated paths, the paths are applied to the white noise and compared with the measured error sensor signal. The outcomes are depicted in figure 4.15. The estimated signal and actual signal, they are matching well, which means the secondary path can be used for the ANC. The estimated secondary path from the adaptive LMS algorithm will be used for the FxLMS algorithm in the next section.

4.3.2 ANC result of second experimental set-up

In the second experiment set-up, the ANC experiments are made also with the single sinusoidal signals of $440Hz$ or $1kHz$ using FxLMS algorithm. The results are shown in figure 4.16 and both sinusoidal signals and some of their harmonics are canceled. Here, the ANC is started in the time signal at 2nd seconds and the $440Hz$ sinusoidal

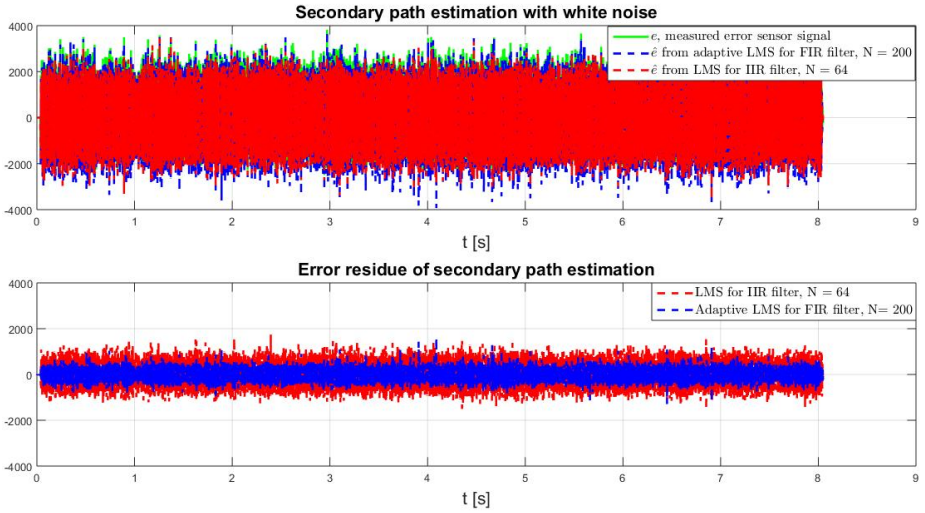

(a)

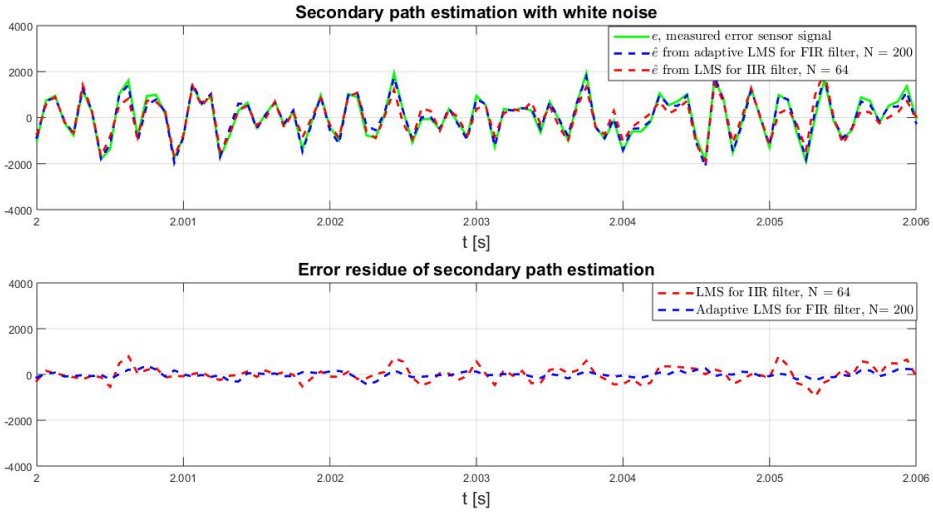

(b)

Figure 4.15: Secondary path estimated with white noise signal. (a) Signal in a full range. (b) Signal in a short range for better visualization.

needed approximately 2 seconds to damp the vibration at the position of the error sensor. Compared to that, the $1kHz$ sinusoidal signal is needed only a half second to damp the vibration. This means, the algorithm is not only dependent from the position of the sensors and shakers, it is also dependent from the signal. During this measurement, the SPL is also measured with the additional microphone and the values are evaluated with FFT in a frequency domain. The result is shown in figure 4.17 and the SPL is decreased by approximately $22dB$ for both sinusoidal signal. This time the SPL is decreased ev-

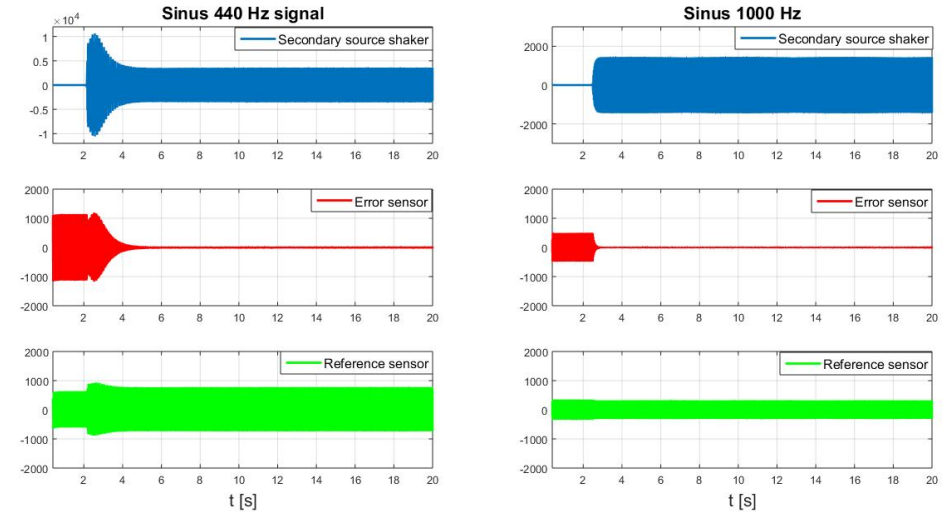

(a)

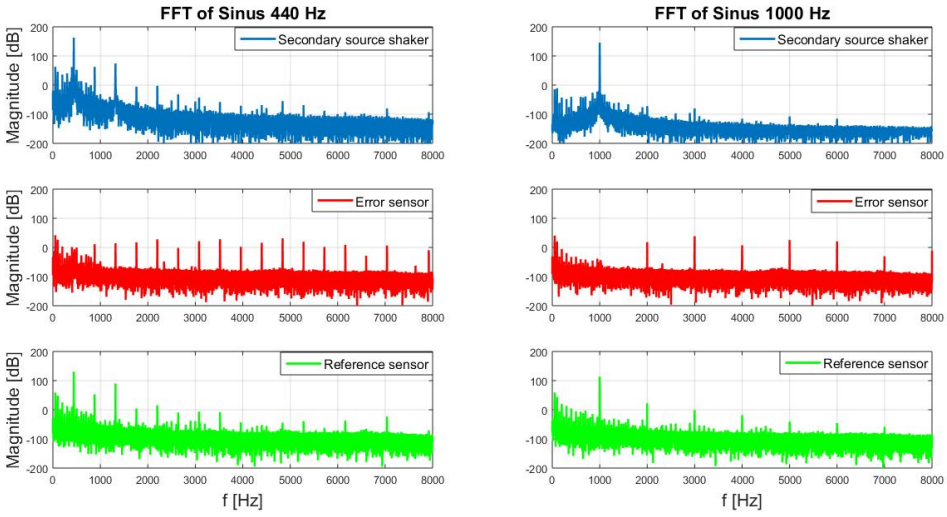

(b)

Figure 4.16: ANC of single sinusoidal signal using FxLMS algorithm. (a) In time domain. (b) In frequency domain.

erywhere and it was not dependent from the microphone position.

Since the FxLMS algorithm is achieved such good result, before testing the system with a real desk signal, the experiment is also performed with multiple sinusoidal signals. The multiple sinusoidal signal contains frequencies of $804Hz$, $960Hz$, $1015Hz$ and $1478Hz$, which are the relevant frequencies to the height desk vibration noise. The error sensor signal and the output signal of FxLMS algorithm are depicted in figure 4.18 in time domain and in the frequency domain. The error sensor amplitude is decreased approxi-

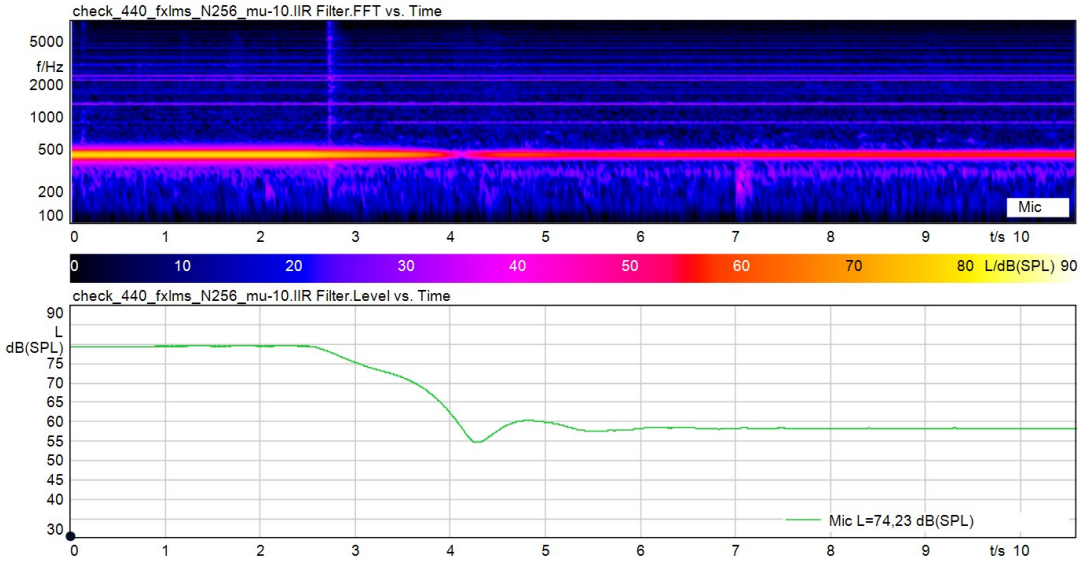

(a)

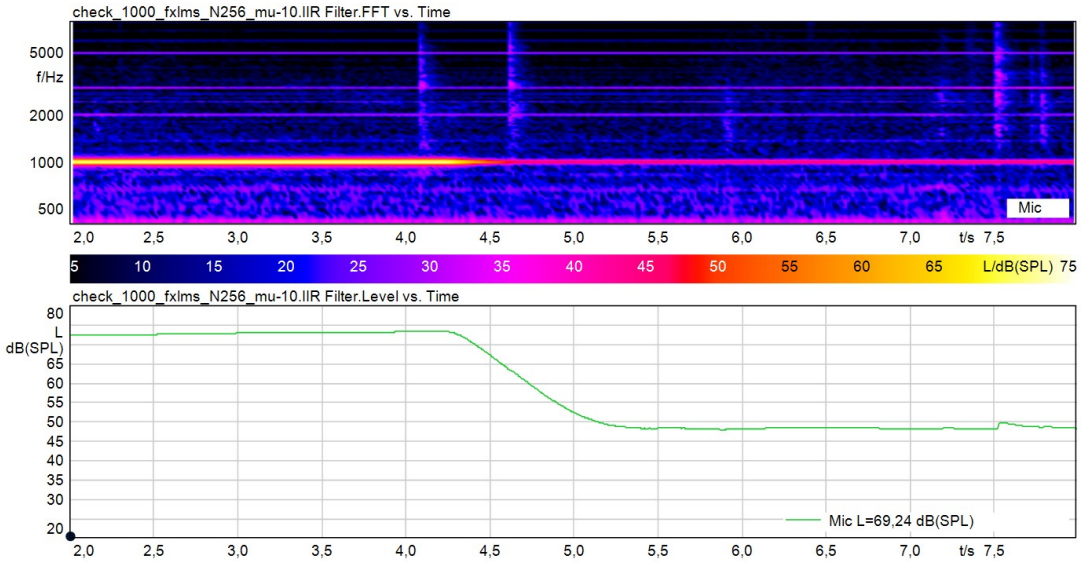

(b)

Figure 4.17: Microphone measurement of sinusoidal signal before and after ANC. (a) $440Hz$ sinusoidal signal. (b) $1kHz$ sinusoidal signal.

mately from 500 to 200 ADC count.

The measurement with microphone is also made during this experiment. The SPL is overall reduced by $10dB$ as shown in figure 4.19. Since the ANC works with the multiple sinusoidal signal, it is expected to work with also a broadband signal. Therefore, the ANC experiment is done with the desk drive signal.

Lastly, the FxLMS algorithm is tested with a desk drive signal. The output signal of

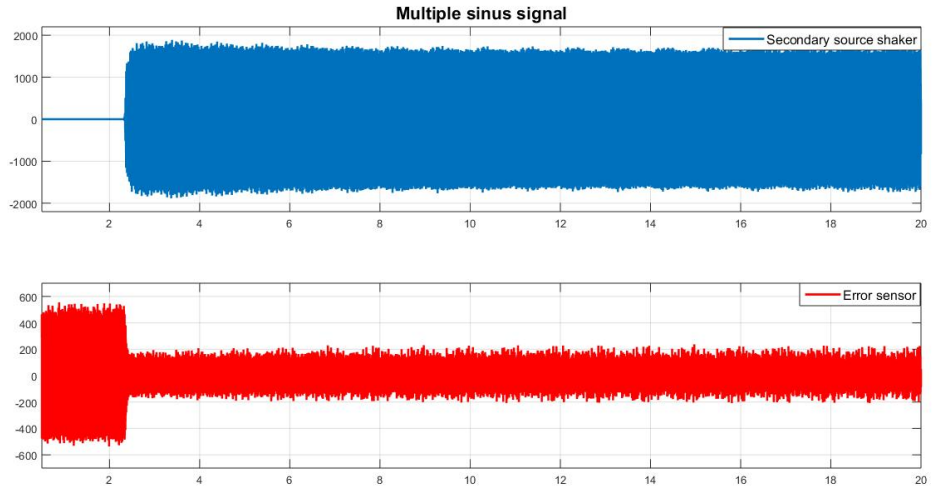

(a)

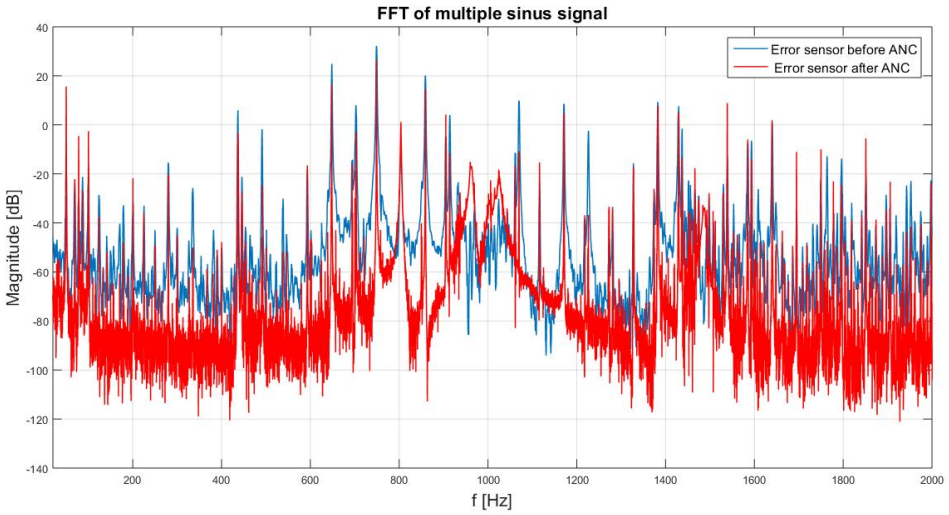

(b)

Figure 4.18: ANC of multiple sinusoidal signal using FxLMS algorithm. (a) In time domain. (b) In frequency domain.

the FxLMS algorithm, error and reference sensor signals are measured and compared before and after ANC is activated. The results are shown in the below figure 4.21 and at the position of the error sensor, the vibration amplitude is decreased in average $20dB$. But the measured SPL from the microphone did not change that much as can be seen in figure 4.20. Overall the SPL from the microphone measurement is decreased by only $2dB$.

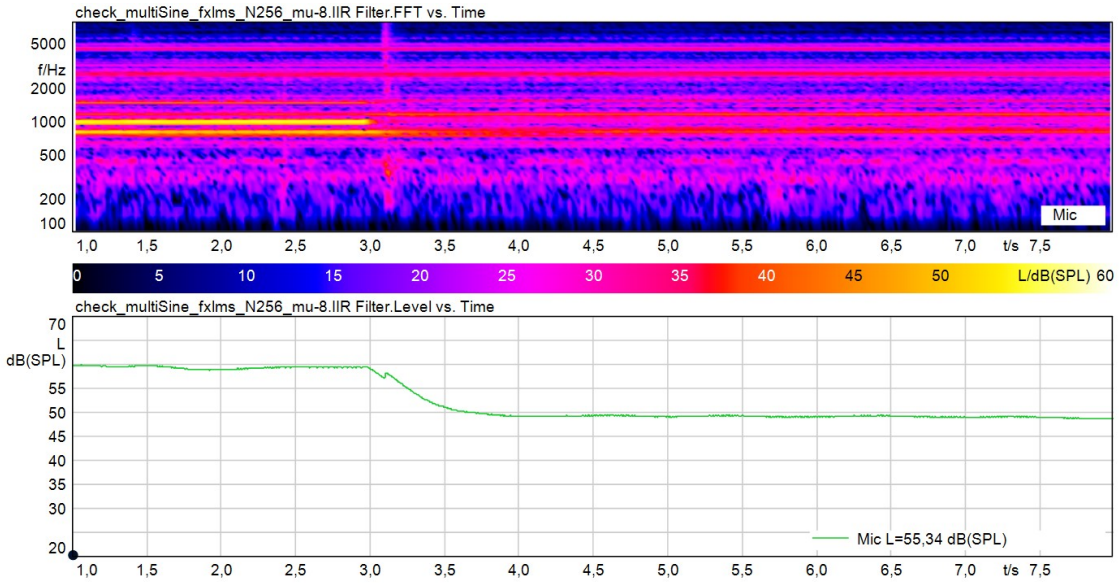

Figure 4.19: Microphone measurement of multiple sinusoidal signal before and after ANC.

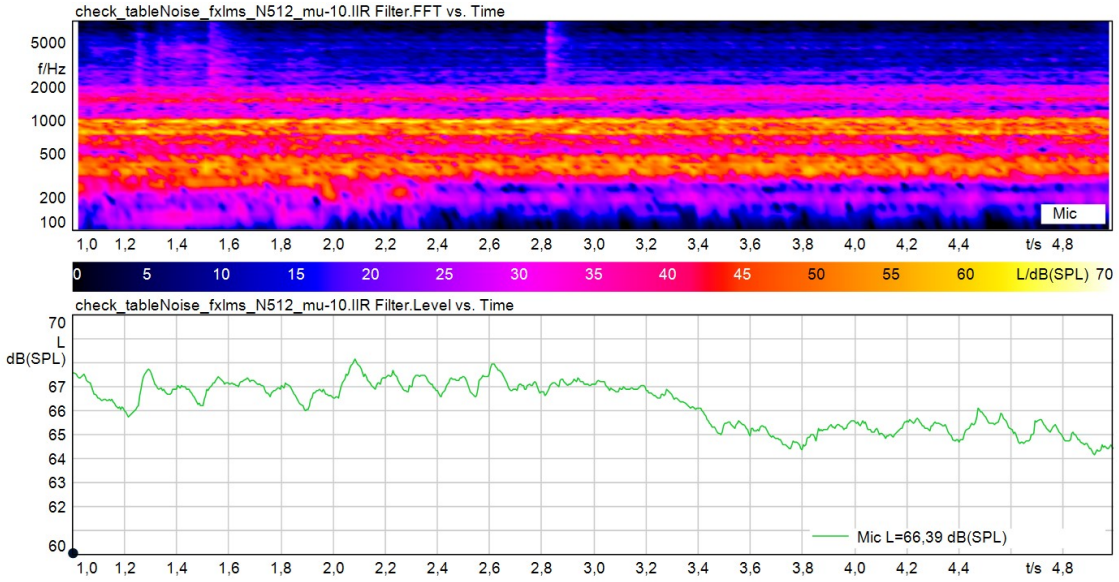

Figure 4.20: Microphone measurement of desk drive signal before and after ANC.

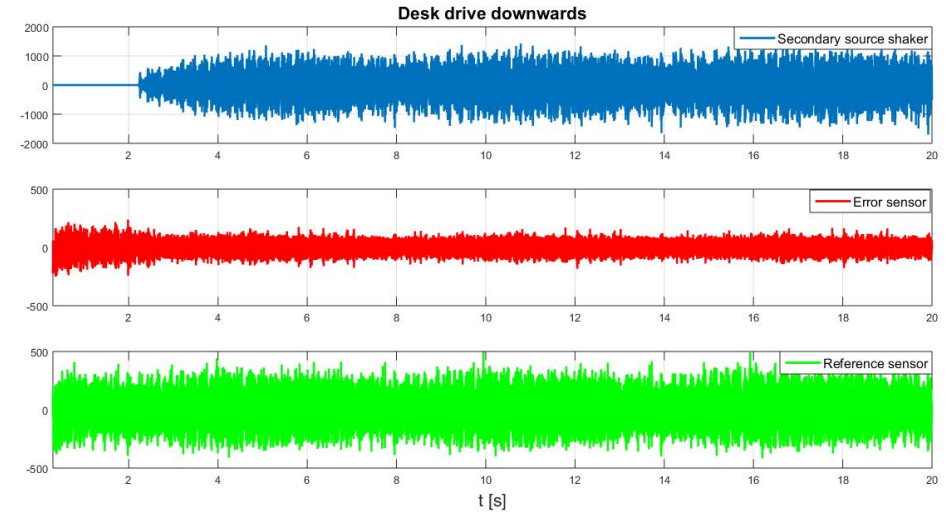

(a)

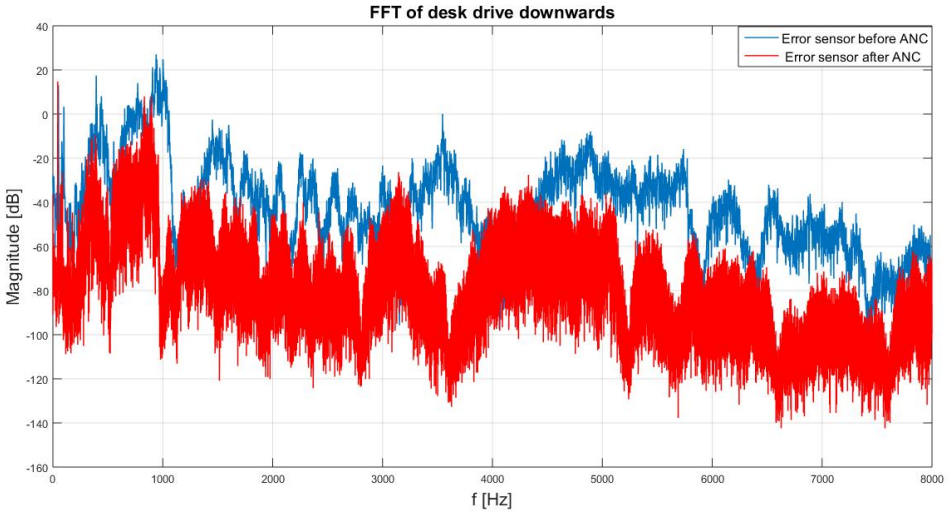

(b)

Figure 4.21: ANC of single sinusoidal signal using FxLMS algorithm. (a) In time domain. (b) In frequency domain.

5 Conclusion and Outlook

5.1 Conclusion

In this thesis, a vibration of a desk plate is damped using an active noise control. The FxLMS algorithm is used as a ANC and the algorithm is implemented and tested with two different experimental set-ups. In the experiment, the vibration is measured with acceleration sensors and the vibrations are generated by 360° vibro-speakers.
The source vibration is created by one of the shakers, which is referred as a primary source shaker. In order to damp this source vibration, the FxLMS algorithm needs a two inputs and one output. The inputs are the acceleration sensors, one of them measures the vibration of the source noise and this sensor is referred as a reference sensor. The other acceleration sensor measures the ANC error residue and it is referred as a error sensor. Based on this two sensor value, the FxLMS algorithm calculates the output, which is the vibration damping signal. This signal is generated by the second shaker and therefore this shaker is named as a secondary source shaker.
A path between the error sensor and secondary source shaker is called as a secondary path. Since the secondary path plays a important role in ANC, the secondary path is estimated with two different algorithms, an adaptive LMS algorithm for FIR filter and a LMS algorithm with IIR filter. The results from the algorithms are verified and both algorithms are estimated the path accurate. However in the experiment, the estimated secondary path using the adaptive LMS algorithm for FIR filter is used because it is easier to implement.
The ANC is applied to different signals, e.g., $440Hz$ and $1kHz$ single sinusoidal signals, multiple sinusoidal signals and a height adjustable desk drive signal. In the first experimental set-up, the FxLMS algorithm was able to damp the vibration of the single sinusoidal signals in the position, where the error sensor is placed. To check overall noise reduction in the room, the radiation of the vibration from the plate in the air, the noise is measured with microphone in different positions. However, the noise was

damped in some position and at the same time it was increased in some other position. The reason is that, the radiation of the vibration is not same every where on the desk plate and it is also highly dependent from the position of the sensors and shakers. To have even radiation of the vibration on the desk plate, the second experimental set-up is introduced.
In the second experimental set-up, the shakers are positioned in the middle of the plate and all the signals as above stated are tested. The vibration of the single sinusoidal and the multiple sinusoidal signals were damped completely in the error sensor position. Overall in the air, the noise was damped by $10dB$ independent from the microphone position. The vibration of the broadband desk drive signal was damped by average $20dB$ in the error sensor position. However, the overall noise is decreased by $2dB$.

5.2 Outlook

The FxLMS algorithm was able to damp the vibration of a narrowband and a broadband signal. The narrowband signals are damped better than the broadband signals. Even though the vibration of the broadband desk drive signal is damped at the error sensor position, the overall noise is decreased only by $2dB$. Therefore, other ANC algorithms, e.g. Filtered-x normalized LMS algorithm and Filtered-u recursive LMS algorithm, can be tested and compare the results that, to check if other algorithms perform better than FxLMS algorithm.
In this thesis, the single-channel FxLMS algorithm is only used. The experiments are performed in the experimental set-ups, therefore the ANC need to be tested with a real application, the height adjustable desk. Since the height adjustable desk contains a two drives, which are mounted on the left and right side of the desk plate, a multiple-channel ANC can be also tested.

A

File Directory

An overview about all of the Matlab-files and Code Composer Studio project-files that were used in this Master Thesis to simulate the algorithms.

Name	Description
myLMS	.m-function to estimate SP using adaptive LMS algorithm offline
identi	.m-function to estimate SP using PI algorithm offline
myRLS	.m-function to estimate SP using PI algorithm online
FIR_calc	.m-script to calculate SP for FIR filter using myLMS function
IIR_calc	.m-script to calculate SP for IIR filter using identi function
IIR_calc_recursive	.m-script to calculate TF for IIR filter using myRLS function

Table A.1: Matlab files

Name	Description
LMS	.c-code to calculate the adaptive LMS algorithm for FIR filter
FxLMS	.c-code to calculate the FxLMS algorithm

Table A.2: Code Composer Studio project-files

List of Figures

List of References

[1] Kuo, S. M. ; Morgan, D. R.: Active Noise Control: A Tutorial Review. In: *Proceedings of the IEEE*, 1999. – ISBN 978–3–540–23159–2, S. 943–973

[2] Lueg, Paul: Process of Silencing Sound Oscillations, 1936

[3] E.Zwicker ; H.Fastl: Psychoacoustics: Facts and Models, Springer-Verlag Berlin Heidelberg, 2007. – ISSN 0018–9219

[4] Frank Fahy, David T.: Fundamentals of Sound and Vibration, Second Edition, CRC Press, 2015. – ISBN 9780415562102

[5] Lin, Yiqing T. ; Abdulla, Waleed H.: Audio Watermark: A Comprehensive Foundation Using MATLAB, Springer Publishing Company, Incorporated, 2014. – ISBN 3319079735, 9783319079738

[6] Kuo, Sen M. ; Panahi, Issa ; Chung, Kai M. ; Horne, Tom ; Nadesk, Mark ; Chyani, Jason: Design of Active Noise Control Systems With the TMS320 Family, Application report. In: *Texas Instrument, Digital Signal Processing Products—Semiconductor Group*, 1996

[7] Fuller, C. R. ; Flotow, A. H.: Active Control of Sound and Vibration. In: *IEEE Control Systems*, 1995. – ISSN 1066–033X, S. 9–19

[8] Sireesha, N. ; Chithra, K. ; Sudhakar, T.: Adaptive filtering based on least mean square algorithm. In: *2013 Ocean Electronics (SYMPOL)*, 2013. – ISSN 2326–5558, S. 42–48

[9] Kuo, Sen M. ; Morgan, Dennis: *Active Noise Control Systems: Algorithms and DSP Implementations*. 1st. New York, NY, USA : John Wiley & Sons, Inc., 1996. – ISBN 0471134244

[10] Olson, Harry F. ; May, Everett G.: Electronic Sound Absorber. In: *The Journal of the Acoustical Society of America* Bd. 25, 1953, 1130-1136

[11] Morgan, D.: An analysis of multiple correlation cancellation loops with a filter in the auxiliary path, 1980. – ISSN 0096–3518, S. 454–467

[12] Homepage of The Company LOGICDATA Electronic & Software, http://www.logicdata.net/blog/product/slimdrive-660s/(accessed on)

[13] Marisol Concha-Barrientos, Kyle S. Diarmid Campbell-Lendrum: Occupational Noise : Assessing The burden of Disease from Work-related Hearing Impairment at National and Local Levels Geneva, World Health Organization. In: *WHO Environmental Burden of Disease Series, No. 9*, 2004. – ISSN 2157–3611

[14] Banbury, Simon ; Berry, Dianne C.: Disruption of Office-related Tasks by Speech and Office Noise. In: *British Journal of Psychology* Bd. 89, Blackwell Publishing Ltd, 1998. – ISSN 2044–8295, 499–517

[15] Miyoshi, S. ; Kajikawa, Y.: Theoretical discussion of the filtered-X LMS algorithm based on statistical mechanical analysis. In: *2012 IEEE Statistical Signal Processing Workshop (SSP)*, 2012. – ISSN 2373–0803, S. 341–344

[16] Barret, Michel: Filter Stability. In: Najim, Mohamed (Hrsg.): *Digital filters design for signal and image processing*. ISTE Ltd, 2006, Kapitel 10

[17] Haykin, Simon: Adaptive filter theory. Upper Saddle River, NJ : Prentice Hall, 2002

[18] Ljung, Lennart (Hrsg.): *System Identification (2Nd Ed.): Theory for the User*. Upper Saddle River, NJ, USA : Prentice Hall PTR, 1999. – ISBN 0–13–656695–2

[19] Isermann, R.: *Identifikation dynamischer Systeme 1: Grundlegende Methoden*. Springer Berlin Heidelberg, 2013 (Springer-Lehrbuch). – ISBN 9783642846793

[20] C. Burgess, J: Active adaptive sound control in a duct: A computer simulation. In: *Journal of The Acoustical Society of America - J ACOUST SOC AMER* Bd. 70, 1981

[21] Elliott, S. J. ; Nelson, P. A.: Active noise control, 1993. – ISSN 1053–5888, S. 12–35

[22] Homepage of Company Thorlabs, https://www.thorlabs.com/newgrouppage9.cfm?objectgroup
on)

[23] Homepage of Company ADIN, http://www.new-adin.com/en/Products/product_35.htmls/(accessed on)

[24] Homepage of Company TE Connectivity, http://www.te.com/global-en/home.html/(accessed on)

[25] TMS320C6713 DSK Technical Reference, Spectrum Digital Incorporated, 2003